CENTER FOR INFRASTRUCTURE ENGINEERING STUDIES

Field Evaluation of Masonry Walls Strengthened with FRP Composites at the Malcolm Bliss Hospital

by

J. Gustavo Tumialan

John J. Myers

Antonio Nanni

Department of Civil Engineering

University of Missouri-Rolla

December 1999

CIES 99-12

Disclaimer

The mission of CIES is to provide leadership in research and education for solving society's problems affecting the nation's infrastructure systems. CIES is the primary conduit for communication among those on the UMR campus interested in infrastructure studies and provides coordination for collaborative efforts. CIES activities include interdisciplinary research and development with projects tailored to address needs of federal agencies, state agencies, and private industry as well as technology transfer and continuing/distance education to the engineering community and industry.

Center for Infrastructure Engineering Studies (CIES)
University of Missouri-Rolla
223 Engineering Research Laboratory
1870 Miner Circle
Rolla, MO 65409-0710
Tel: (573) 341-6223; Fax -6215
E-mail: cies@umr.edu
www.cies.umr.edu

Field Evaluation of Masonry Walls Strengthened with FRP Composites at the Malcolm Bliss Hospital

by

J. Gustavo Tumialan

John J. Myers

Antonio Nanni

Department of Civil Engineering

University of Missouri - Rolla

Report No. CIES 99-12

Center for Infrastructure Engineering Studies

University of Missouri - Rolla

ABSTRACT

Masonry walls at a decommissioned building in St. Louis, Missouri were tested to failure. The walls were subjected to out-of-plane loading and in-plane loading. Previous work on URM and reinforced masonry walls strengthened with FRP laminates has shown remarkable increases in capacity and ductility. However, most of this research has been conducted under laboratory conditions, where, many times, it is a difficult task to represent real field conditions. In this context, this experimental program on out-of-plane loading offered a singular opportunity for performing field experimentation on URM walls strengthened with Glass, Aramid and Carbon Fiber Reinforced Polymers (GFRP, AFRP and CFRP, respectively) composites. Parameters such as the type of composite system, strip width, and FRP installation methods were evaluated. A mechanism of failure caused by a shear-compression effect lead to the fracture of either the upper or lower boundary masonry units. Due to this failure mode, the walls were not able to develop a higher capacity compared to the control specimen.

For in-plane loading the test results demonstrated that near-surface-mounted rods confined to the toe region of the walls were able to increase the capacity of the wall as well as to provide a pseudo-ductile behavior to the masonry system.

TABLE OF CONTENTS

LIST OF ILLUSTRATIONS

LIST OF TABLES

1. INTRODUCTION

1.1. PROJECT BACKGROUND

The old City Hospital complex in St. Louis, Missouri was decommissioned and scheduled for demolition. Before the demolition takes place, one of the buildings, the Malcolm Bliss Hospital, was used as a research test bed (see Figure 1.1). The building of interest, a five-story reinforced concrete-frame addition built in 1964, has in its contour Unreinforced Masonry (URM) Walls and reinforced parapets, which were tested under out-of-plane and in-plane loading.

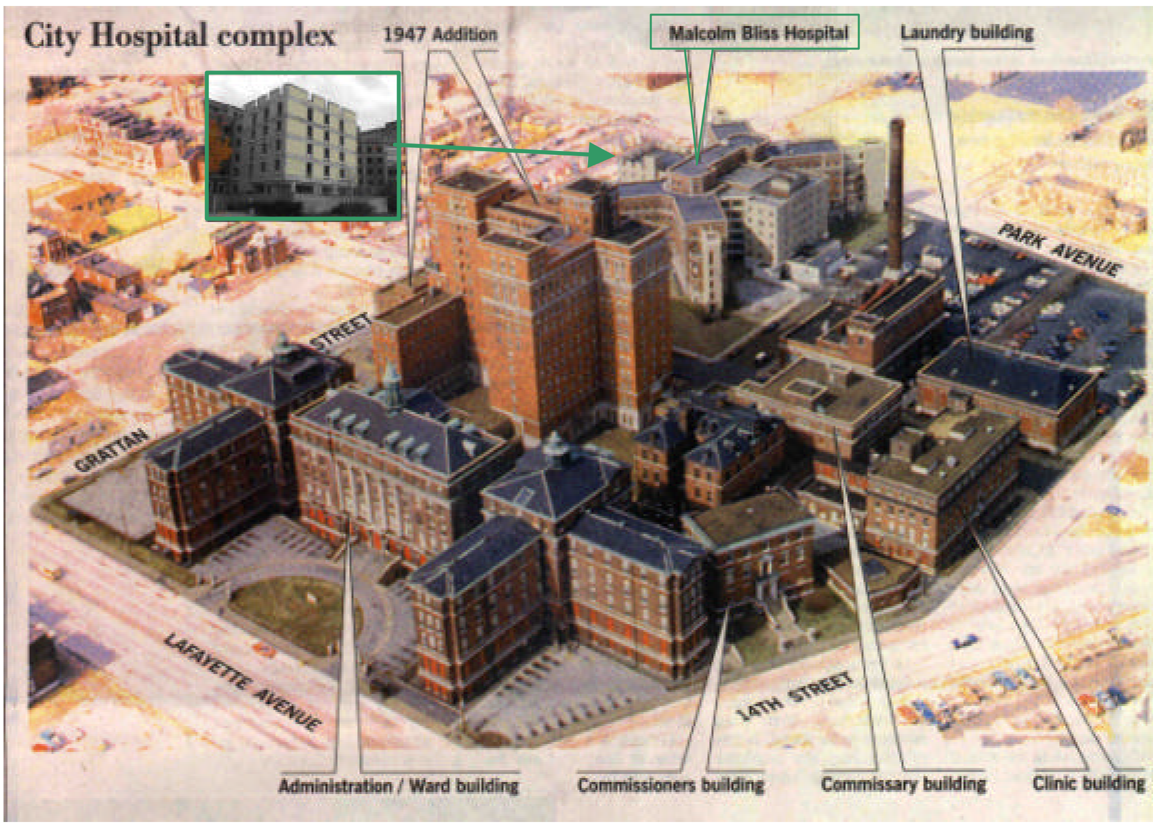

Figure 1.1. City Hospital complex – St. Louis, MO

Source: St. Louis Post Dispatch

Structural weakness or overloading, dynamic vibrations, settlement, and in-plane and out-of-plane deformations can cause failure of masonry structures. Although, most of the research on FRP has been focused on reinforced concrete, available literature on masonry shows that each of these causes can be prevented and/or lessened by using FRP composites. Previous research investigations on FRP composites (tendons and laminates) have included variables such as prestressing, temperature effects, various types of loading and strengthening conditions, as well as anchorage systems.

Unreinforced masonry (URM) walls can be either load bearing or infill walls, which are primarily constructed with solid and hollow clay brick. Due to weak anchorage to adjacent concrete members, for the case of load bearing walls, or due to absence of anchorage for the case of infill walls, URM walls may tear and collapse under out-of-plane loads generated by seismic forces, as illustrated in Figure 1.2. According to organizations such as The Masonry Society (TMS) and the Federal Emergency Management Agency (FEMA), failures due to out-of-plane bending in URM walls result in most of the material damage and loss of human life. Thereby, the development of effective strengthening techniques to address out-of-plane bending is of interest.

Figure 1.2. Out-of-Plane Failure

Source: Northridge Collection, Earthquake Engineering Research Center, University of California, Berkeley

Reinforced masonry walls are usually part of "box system" structures, in which walls resist gravity load, and in-plane loads. The latter caused by either a seismic event or high wind load. Depending on the structural configuration of these members, such as effective aspect ratio of the wall components, and amount of vertical and horizontal reinforcement, two mechanisms of failure can be observed. One is an in-plane flexural failure, which is characterized by tensile yielding of vertical reinforcement and/or crushing of masonry in the area of the toe wall. The second mechanism is a shear failure, characterized by diagonal tensile cracking, which is illustrated in Figure 1.3.

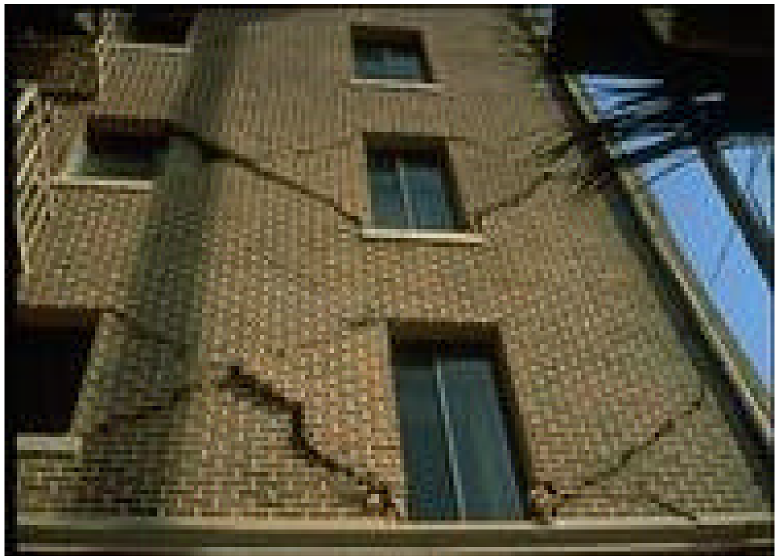

Figure 1.3. Diagonal Tensile Cracking

Source: Northridge Collection, Earthquake Engineering Research Center, University of California, Berkeley

Conventional retrofitting techniques can be classified according to the problem to address: damage repair or structure upgrading. For damage repair in the form of cracks the following methods can be used:

- Filling of cracks and voids by injecting epoxy or grout.
- Stitching of large cracks and weak areas with metallic or brick elements.

For strengthening or upgrading the following procedures are available:

- Grout injection of hollow masonry units with non-shrink portland cement grout or epoxy grout to strengthen or stiffen the wall.
- Construction of an additional wythe to increase the axial and flexural strength.
- Post-tensioning of an existing construction.
- External reinforcement with steel plates and angles.
- Surface coating with reinforced cement, such as a welded mesh.

Without highlighting the importance of a lower installation cost the use of FRP composites, made of carbon, glass and aramid fibers, their use possesses some advantages compared to the traditional methods mentioned above. For example, the disturbance of the occupants of the facility is minimized and there is minimal loss of usable space during strengthening. Furthermore, from the structural point of view, the dynamic properties of the structure remain unchanging because there is no addition of weight and stiffness. Any alteration to the aforementioned properties would result in an increase in seismic forces.

1.2. SCOPE AND OBJECTIVES

Previous works on URM and reinforced masonry walls strengthened with FRP laminates have shown remarkable increases in capacity and ductility (Velazquez, Ehsani, and Saadatmanesh, 1998). However, most of this research has been conducted under laboratory conditions, where in many times the conditions are not representative of field conditions conditions. In this context, the tests performed at the Malcolm Bliss Hospital offered the opportunity for performing field experimentation on masonry walls strengthened with Glass, Aramid and Carbon Fiber Reinforced Polymers (GFRP, AFRP and CFRP, respectively), as well as Glass Rods. As part of this study two experimental programs were conducted. The first experimental program dealt with URM walls strengthened with FRP composites subjected to out-of-plane loading. Parameters such as the type of composite system, strip width, and FRP installation methods were evaluated. A mechanism of failure caused by a shear-compression effect lead to the crushing of either the upper or lower masonry units. Due to this kind of failure, the walls were not able to develop a higher capacity compared to the control specimen.

The second program was on reinforced masonry walls strengthened with FRP composites under in-plane loading. Different strengthening schemes, as well as the effect of openings were investigated. Flexural-controlled failures were observed as a result of the tests.

The chief objective of these programs is to evaluate the effectiveness of different types of commercially available and experimental forms of fiber reinforced polymer (FRP) composite systems (i.e. near-surface-mounted rods) to increase flexural and shear capacities of masonry elements.

Static load tests to failure were carried out as part of the experimental programs. The goal of the static load test evaluation is to assess the performance of structural and non-structural members before and after strengthening with composite systems. The load testing procedure involves applying concentrated loads to the walls. Their response was monitored and used for their evaluation.

2. LITERATURE REVIEW

2.1. MASONRY UNITS IN BACKUP WALLS

In Section 4, it will be shown that masonry units constituting the backup walls controlled the behavior of the two-wythe walls tested under out-of-plane loading. Thereby, it is important to identify the units, since they may govern the wall behavior.

Commonly two different masonry units are found in backup or inner walls, clay tiles and concrete units. Structural clay tile has been first manufactured in the United States approximately since 1875. A clay tile is a hollow unit, is characterized by possessing parallel cores and thin webs and faceshells. In the beginning, structural tile was used in building floors and as a fireproofing material for steel frame construction. Owing to its lightweight characteristics, large unit size and ease of construction, the use of clay tiles was extended to load-bearing walls, wall facings, silos, columns, etc. In the early 1900's, structural clay tiles were used in infill walls throughout the United States. Some notable structures were it is possible to observe this kind of construction are the New York Chrysler Building, Los Angeles City Hall Building, and The Oakland City Hall Building in California, which is considered a historic structure.

Figure 2.1 illustrates information, available in the U.S. Department of Commerce Census of Manufacturers, on the production of clay tile in the 20th century. As can be observed, the maximum peak in the production of clay tiles was in the 1920's. As a consequence of the Great Depression, the production suffered a dramatic decrease. As World War II began, the economy was revitalized and large public works were performed. Some of military facilities built primarily with clay tiles included Fort Benning in Georgia, and the Women's Army Auxiliary Corps Barracks in Iowa. From the same figure, it is observed that the production of clay tiles decreased during the 1960's, when concrete units began to be widely used.

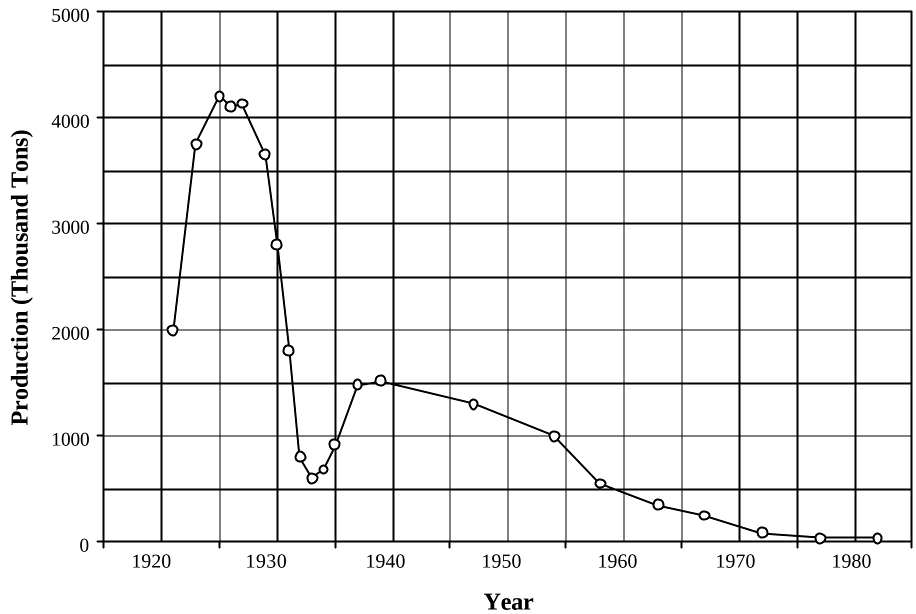

Figure 2.1. Production of Clay Tile during the 20th Century

This change in the market was due to a high production capability of concrete blocks, which led to low unit cost and increased available quantity. In addition, the manufacturing process of concrete units allowed a better quality control of the products. For instance, concrete units show more uniformity since they are not fired during their manufacture process. Also, due to the brittle characteristics of clay tiles when being handled and transported, made that the demand of concrete units was increased. Another cause for the decrease of clay tiles production was the efforts driven by the Environmental Protection Agency (EPA) to reduce the environmental costs associated with the manufacture of masonry units. This led to the closing of many old plants where the kilns generated emissions above the standards.

However, the use of concrete units was not new in the United States, they were first manufactured in the United States at about the turn of the 20th century in small one-at-a-time machines that could be operated by hand and purchased from Sears and Roebuck catalogs. Due to this manufacturing limitation and because the architects preferred the use of stone because of its integrity, the use of concrete units was limited.

2.2. RETROFITTED MASONRY WALLS

Existing masonry buildings around the world, many of which are of historical and architectural value, do not meet current building codes. In fact many of these buildings have suffered the effects of seismic and wind loads, foundation settlements, or environmental deterioration, which leads to their retrofit and strengthening. In the following sections some studies on masonry walls retrofitted with conventional methods and with FRP composites are briefly described.

2.2.1. Masonry Walls Retrofitted with Conventional Methods. Two studies dealing with conventional methods to retrofit and upgrade masonry structures are described herein. *Prawel et al. (1985)* investigated masonry panels retrofitted with ferrocement overlays. Ferrocement is an orthotropic composite material, which consists of a high-strength cement mortar matrix and layers of fine steel wires configured in the form of a mesh. These overlays are used to increase in-plane and out-of-plane resistance. The study focused on masonry walls subjected to in-plane loading. Two modes of failure were observed; a ductile one caused by diagonal tension and a brittle failure caused by debonding of the ferrocement overlay. The experimental results indicated that the strength and ductility were almost doubled in the coated walls compared to the control walls.

Manzouri et al. (1996) conducted a comprehensive study to evaluate the efficiency of repair for URM walls by grout injection and in combination with horizontal and vertical steel reinforcement. Stainless steel with a helical design was used as the reinforcement. The specimens had grout injection as a part of the repair and retrofit process. The installation procedure included cutting of certain bed joints to a depth of 3-in., followed by placement of the tie in the slot and sealing with mortar. The walls, which were tested under in-plane loading, exhibited that the injection of grout accompanied by repair of localized damaged areas can restore the original strength and stiffness of control walls. The introduction of horizontal reinforcement increased the strength and ductility of the wall system, by preventing an initial shear failure was avoided. Consequently, the vertical reinforcement increased the lateral resistance and ductility.

2.2.2. Masonry Walls Retrofitted with FRP Composite Systems. *Schwegler et al. (1995)* investigated strengthening methods for masonry shear walls corresponding to the lowest building story. The goals of this research study were to increase the system ductility, generate uniform crack distribution, and increase the load carrying capacity of the system. Two methods of strengthening were investigated. In the first method, CFRP sheets were bonded diagonally to masonry shear walls and anchored in the adjacent boundary elements which consisted of ceiling and floor slabs. In the second method, conventional woven fabric was attached to the entire wall surface. In this case the fabric was not anchored to the adjacent concrete structures. Some test observations to highlight were that the strengthened shear wall exhibited elastic behavior up to 70% of the maximum shear force. Also, the carrying capacity decreased as a consequence of massive crack formation in the masonry. In the walls strengthened with CFRP sheets, the deformation was increased; however, due to delamination of the CFRP sheets from the masonry, significant increases in the carrying capacity compared to walls strengthened with conventional woven were not observed. It was observed that if only one side of the masonry wall is strengthened, the capacity could be halved. In addition, the eccentricities caused by this strengthening scheme had a minimum effect on the shear carrying capacity.

Laursen et al. (1995) performed shear and flexural tests on masonry walls strengthened with carbon overlays. In the case of the shear tests the primary objective was to change the mode of failure from a brittle failure to a ductile failure. For the flexural wall test, the goal was to investigate the behavior of different strengthening schemes. For the shear test specimens, it was observed that the presence of carbon overlays improved the wall performance by changing the failure from a shear failure mode to a flexural failure mode. This change in the mode of failure caused an increment in ductility of approximately 100%, and prevented a brittle failure mode. The flexural program made possible to observe the achievement of larger capacities and ductility levels compared to walls with essentially no flexural strength. The failure was caused by rupture of carbon overlays.

Schwegler et al. (1996) carried out a retrofitting project carried out in Switzerland, where two sixty-year old, six-story buildings were reclassified for use. As a consequence, some load bearing walls had to be strengthened in order to resist potential earthquakes. CFRP sheets were attached in a cross-wise fashion to one side of masonry walls. The sheets were anchored to reinforced concrete (RC) slabs by means of bolts, below the wall. Previous research conducted by one of the authors showed that only the strengthening of one side of the wall was required. The design calculations to determine the strength of the retrofitted wall were done according to the Stress Fields Theory.

Hartley et al. (1996) reported the feasibility of using CFRP sheets for repairing block walls used in residential construction due to settlement. Test specimens were subjected to a simulated foundation settlement. The settlement loads were similar to the cantilevered weight of the walls. Their dimensions were 8 ft. high, 20 ft. long and 8 in. thick. Since the carbon fiber was intended to increase the bending resistance, it was oriented parallel to the bed joints, and attached to only one side. By comparing the control wall and the retrofitted wall an increase over 80% was observed.

Ehsani et al. (1998) investigated the flexural behavior of URM walls with GFRP sheets. Small URM beams were tested to failure under static loading of two concentrated loads. The beams were 8.5-in. wide, 4-in. high, and 57 in. long. The primarily failure was a tension failure, which was observed when relatively weak strengthening was used. When the number of plies was increased, the failure mode of changed to compression of the brick. I was observed that the flexural capacity was increase up to 24 times compared to the control beam.

Muszinsky et al. (1998) performed explosive field tests on masonry walls strengthened with composite materials. Infill walls, 100 in. wide, 112 in. high, and 8 in. thick were tested under air blasting loading at a standoff distance of 95 ft. The control wall exhibited a 7.5-in. displacement at the midheight; at the final stage spalling of the front face occurred throughout the masonry section. All the mortar joints failed due to the blast load; however, an arch between two center blocks avoided the breaching of the wall. For the strengthened wall, the unprotected structure fissured and the concrete frame displaced 2 in. Considerable spalling was observed on the front face. The wall exhibited 0.12-in. residual displacement at the midheight, much less than the control specimen.

Velazquez et al. (1998) reported test results of two half-scale single wythe URM walls tested under out-of-plane cyclic loading. The test specimens were 48 in. wide and

1.92 in, having each wall different height; thus two different slenderness ratio h/t, 14 and 28, were investigated. The walls were strengthened on both faces with GFRP strips. The slender wall was strengthened with the same amount of FRP on both faces; whereas, the short wall was strengthened with different amounts of FRP on the faces. Tensile failure of the reinforcement was observed in the slender wall. Delamination of the GFRP sheets was the controlling factor in the short walls. Substantial increases in strength and ductility was achieved. It was observed that the short and slender wall supported lateral pressures equivalent to 31 and 13 times their weight, respectively.

2.3. FINAL REMARKS

The use of FRP composites for retrofitting masonry structures offers some advantages compared to the use of conventional retrofitting techniques. As an example, FRP composites do not add considerable mass to the structure. This extra weight can modify the dynamic response to seismic events, which may be observed by using masonry-RC composite walls or ferrocement overlays. From the architectural point of view, the use of conventional methods may violate the aesthetics of building facades. In addition, due to their labor characteristics, they may intrude on usable space adjacent to strengthened components. The aforementioned facts along with the outstanding properties of FRP materials make the use of FRP composites attractive for strengthening of masonry structures.

Studies on masonry walls strengthened with FRP composites have shown that increases in either out-of-plane or in plane capacities as well as ductility can be achieved. However, most of these studies have been carried out in laboratories, under ideal conditions such as considering free rotation in the supports. In this sense, the tests performed for the present research offered an opportunity to test walls under real boundary conditions. They allowed observing other factors, such as the effect of upper and lower beams, and plaster delamination, which are not commonly reproduced in the laboratory.

3. MATERIAL PROPERTIES AND INSTALLATION TECHNIQUES

3.1. MASONRY

One inherent difficulty when conducting a testing program in situ is to characterize the materials. In order to attain this task, samples obtained from similar walls in the building were collected. These samples included bricks, tiles, and mortar. Due to their brittle characteristic, it was not possible to recover any masonry assemblage from the interior wall. However, in the case of the veneer wall some assemblages consisting of two courses of bricks were attained for laboratory analysis. The compressive strength of these assemblages was 1300 psi.

The compressive strength of the inner wall bricks was 266 psi, whereas the compressive strength of the mortar was 814 psi. It is important to mention that the latter value was not obtained from standard tests, but from cylinder shaped mortar entrapped in the cores of the brick veneer. Using the average compressive strength, the mortar can be classified as Type N according to the ASTM C270.

3.2. COMPOSITE SYSTEMS PROPERTIES

FRP sheets and rods were used in this research study to strengthen in-situ masonry walls. For the FRP sheets the system consisted of three basic components, namely: putty, saturant and fiber sheets. The combination of these three materials forms the FRP laminate. For the near-surface-mounted-rods, the system consisted of two components: a concresive paste and rods. The properties of the putty and saturant are illustrated in Table 3.1.

Table 3.1. Resin Properties in Tension

Material	Stress at Yield (psi)	Stress at Rupture (psi)	Strain at Yield	Strain at Rupture	Elastic Modulus (psi)	Poisson's Ratio
Putty	1900	2100	0.020	0.070	260,000	0.48
Saturant	7800	7900	0.025	0.035	440,000	0.40

It is important to highlight that for strengthening of masonry walls, the surface is primed with the saturant used to impregnate the fibers rather than the conventional primer used for concrete surfaces. Three types of commercially available FRP sheets, GFRP, AFRP and CFRP, as well as Glass Rods were used to strengthen the walls. Their engineering properties are summarized in Table 3.2.

Table 3.2. Engineering Properties for FRP Sheets and Glass Rods

Material	**Design Strength (ksi)**	**Design Tensile Modulus (ksi)**	**Load per Sheet Width (lb/in)**
GFRP - EG900	220	10,500	3050
AFRP – AK 40	290	17,000	3190
CFRP – CF 130	550	33,000	3580
E-Glass Rods	121	6,000	------

3.3. COMPOSITE SYSTEMS INSTALLATION TECHNIQUE

The strengthening of masonry walls consisted of applying FRP composite materials made of strong fibers such as carbon, glass and aramid bound together by an epoxy resin matrix, as well as the installation of near-surface-mounted glass rods.

The FRP sheets were attached to the wall surface by manual lay-up, for their installation a procedure recommended by the manufacturer was followed. This task was carried out for a qualified contractor.

Since the performance of the composite materials relies on bonding, surface preparation was an important issue to be accomplished before installation of the sheets. Two installation methods were used depending on whether the FRP was bonded to a plaster surface or directly to the masonry surface. In the first case, two procedures were investigated. For the sake of discussion they are called Procedures A and B:

Procedure A: The paint and paris layers were removed using a grinder with a $4^{1}/_{2}$” diamond blade. In terms of surface finishing this procedure gave good results, since not excessive exposition of the aggregates present in the plaster was observes, as illustrated in Figure 3.1. A main disadvantage of this procedure was the preparation time, which for large scale projects may not be practical.

Procedure B: The surface was prepared by means of sandblasting, which was performed using an abrasive blast machine with a 300 lbs. sand capacity. This procedure was less labor intensive than the previous; however, due to the lack of control to measure the aggregate exposure during the sandblasting, the aggregates were excessively exposed, requiring a larger amount of putty to level the surface (see Figure 3.1).

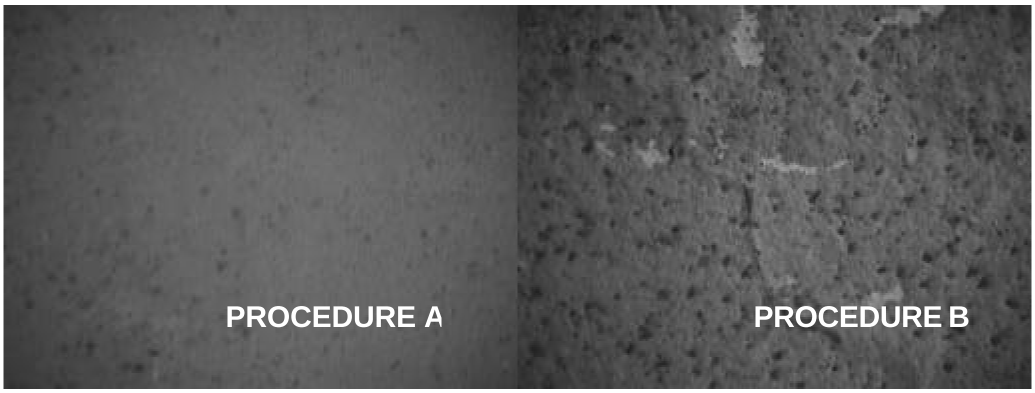

Figure 3.1. Aggregates Exposure

It may be concluded that each of these methods had pros and cons. The final adopted procedure was a combination of procedures A and B, and which can be summarized as follows: sandblasting was employed to remove most of the paris layer; next the surface was finished with grinding (see Figure 3.2).

Figure 3.2. Grinding of Wall Surface

For FRP installation on bare masonry walls, the following was undertaken. After sandblasting the surface (see Figure 3.3), the excess of mortar joints was eliminated using a grinder with the objective of obtaining a leveled surface. This is illustrated in Figure 3.4.

Figure 3.3. Surface Sandblasting

Figure 3.4. Removal of mortar excess in bed joints

In both cases the dust originated by the preparatory tasks was removed from the wall surface using air pressure before the installation of the FRP sheets. The installation of the FRP sheets can be summarized as follows:

- Epoxy saturant was applied as primer to fill cavities on the masonry wall surface. The constituent parts of the saturant usually have some particles settled on the bottom of the recipient; therefore, they were premixed independently using a 4" mixing jiffy paddle prior to obtain the final mix. The constituent parts were mixed during three minutes time intervals, according to a proportion specified by the manufacturer, using a 2" mixing jiffy paddle.

- The primary purpose of using putty was to level the uneven surfaces present on the wall surface (see Figure 3.5). After the putty set, the surface was smoothed to eliminate irregularities on the surface. This was carried out using a grinder.

Figure 3.5. Putty Application

- A layer of saturant was applied to the surface using a roller. Following this, the FRP sheets were adhered to the wall surface. (see Figure 3.6)
- The FRP sheets were then cut to the required length. Once, the sheet was placed, it was press down using a "bubble roller", which eliminates the entrapped air between the saturant and fibers. Finally, a second layer of saturant was applied as shown in Figure 3.7.

Figure 3.6. Fibers Installation

Figure 3.7. Saturant Impregnation

For the walls where near-surface-mounted rods were installed, the procedure can be summarized as follows: lines of ¾" wide were drawn on the wall at the desired location as guidelines for the specified width of the grooves. By using a grinder with a diamond blade, slots were then grooved, as illustrated in Figure 3.8. The plaster and masonry material was then removed using chisel and hammer completed the slots. For the test walls where rods were anchored to RC members, 8 in. deep holes were drilled using a hammer drill with a ¾" bit. Once the drilling of holes was completed, the dust was removed from their interior by means of an air blower.

Figure 3.8. Grooving of Slots

A concresive paste was used to provide bond between the masonry and the rods. First, using a mason trowel, a layer of paste was placed into the slots. Following this, a rod was nested in the slot (see Figure 3.9). The slot was then completely filled with the paste to encapsulate the rod. In the case of rods anchored to RC members, the holes were previously filled with paste using an injecting gun.

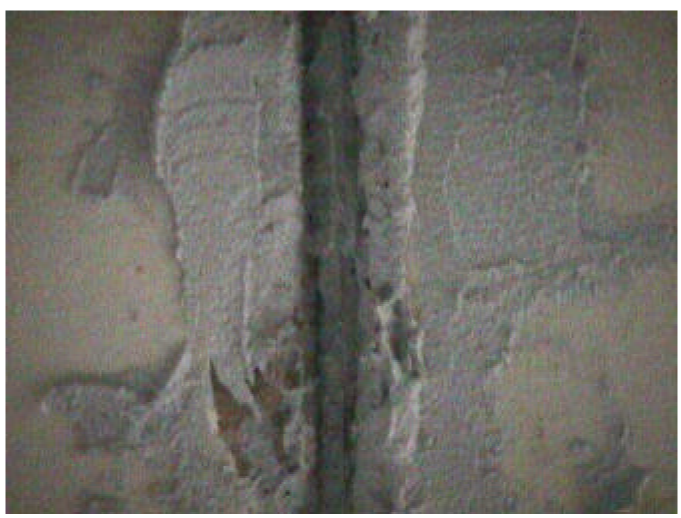

Figure 3.9. Near-surface-mounted rod nested in concresive paste

4. EXPERIMENTAL PROGRAM

4.1. OUT-OF-PLANE WALLS EXPERIMENTAL PROGRAM

4.1.1. Test Specimens. Ten full-scale URM walls, constructed of clay units, were tested. The nominal dimensions of these walls were 8x 8 ft.; their overall thickness, including the two wythes and plaster was 13-in. The upper and lower boundaries for these walls were RC beams which were cast integrally with the floor system. The studied walls, classified as infill, belong to a masonry typology commonly used during a time frame from late 1940's through the early 1960's. A section view of a typical wall is shown in Figure 4.1. The walls under investigation consisted of two wythes of masonry units spaced at ¾", joined only by header units placed at each fourth course, and at each fourth unit in the course in mention. The outer wythe, corresponding to the veneer wall, was built using cored units with the following physical dimensions, 3.75 in. wide, 2.25 in. high and 8 in. long, the units had three cores of 1.5 in diameter. The inner wythe or backup wall was constructed using two kinds of clay units. Tiles and bricks were laid in alternated courses, as can be observed in Figure 4.1. The actual dimensions of the tile units were 7.5 in. wide by 7.5 in. high by 12 in. long. The brick units were solid, their dimensions were 4.25 in. wide, 2.25 in. high and 8.5 in. long. The walls were finished with one-inch thick cementitious plaster, reinforced with a two-directional welded steel mesh at mid-depth.

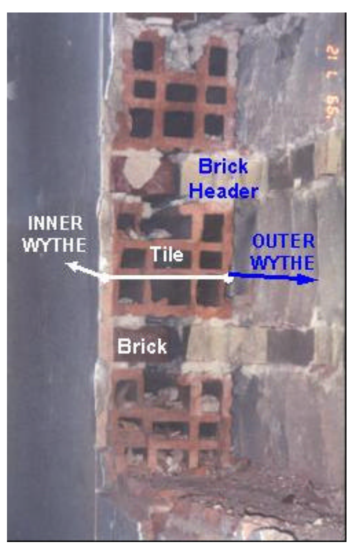

Figure 4.1. Vertical Cross Section of Typical Wall

A summary of the experimental program is shown in Table 4.1; also, the typical strengthening schemes are shown in Appendix A. Two URM walls, Wall 1 and Wall 2, were selected as control specimens. In Wall 1 the plaster remained on its surface; whereas, in Wall 2 the plaster was removed to differentiate the impact of the cementitious plaster. The remaining specimens were strengthened with different composite materials, namely GFRP, AFRP, CFRP and deformed GFRP rods. Thus, Wall 3 was strengthened with three 20-in. wide GFRP strips attached to the plaster surface. The strengthening scheme for Wall 4 was similar to that of Wall 3, except that the GFRP strips were applied directly to the masonry, meaning without the presence of plaster. The purpose of testing this group of walls was to observe the difference in behavior, if any, in walls strengthened with FRP attached to plaster and to masonry under out-of-plane loading. One of the advantages of using composite materials is that little disruption is caused during its installation. That was the purpose of studying the behavior of walls strengthened without the removal of plaster. Thus, in the remaining walls the strengthening was carried out with the presence of plaster.

Wall 5 was strengthened with three 10-in. wide GFRP strips, with the purpose of comparing it to Wall 3, which had twice amount of reinforcement. In Wall 6 and Wall 7 the strengthening geometry was similar to Wall 3. In the first case the URM wall was strengthened with AFRP; whereas, in the latter case CFRP was used as strengthening material. Wall 8 was strengthened using two different composite systems: GFRP sheets and near-surface-mounted GFRP rods. Four #3 pieces with a length of 26 inches, two in each end, were placed under each strip of GFRP. With the purpose of providing continuity to the GFRP sheets, the rods were anchored to the RC beams, with a development length of 8 in.

The fact that the anchorage of near-surface-mounted rods into adjacent RC members (i.e. slabs, columns and beams) is a feasible task, makes attractive their use for increasing the flexural strength of masonry walls. Thereby, Wall 9 and Wall 10 were strengthened with eight #3 GFRP rods spaced at 12 in. In the first case the rods were not anchored to the adjacent beams; whereas, in the latter case the rods were anchored 6 in. into the upper and lower beams. The purpose of testing these walls was to compare their behavior to those of walls strengthened with composite sheets, as well as observe the behavior of anchored rods and non-anchored rods.

Table 4.1. Experimental Program for Out-of-Plane Walls

Specimen	Strengthening System	Reinforcing Scheme	Plaster
Wall 1	Control	None	Yes
Wall 2	Control	None	No
Wall 3	GFRP Sheets	Three strips (width=20 in)	Yes
Wall 4	GFRP Sheets	Three strips (width=20 in)	No
Wall 5	GFRP Sheets	Three strips (width=10 in)	Yes
Wall 6	CFRP Sheets	Three strips (width=20 in)	Yes
Wall 7	AFRP Sheets	Three strips (width=20 in)	Yes
Wall 8	GFRP Rods and GFRP Sheets	Three strips (width=20 in), anchored with rods	Yes
Wall 9	GFRP Rods	Eight #3 near-surface mounted rods	Yes
Wall 10	GFRP Rods	Eight #3 anchored near-surface mounted rods	Yes

4.1.2. Test Setup. The masonry walls were tested under two out-of-plane loads, which were distributed by 12 x 12 x ½-in. steel plates to the external face of the wall (see Figure 4.2).

Figure 4.2. Plates on the external face of the wall

The loads were generated by means of a 200 kip hydraulic jack using a manual pump. The force created by this jack reacted against a five foot steel girder made of two C10x20, hereafter called Beam A, and an 11 foot steel girder made of two C15x40, hereafter referred as Beam B. When loading, two reacting forces were created on Beam A. These forces were transmitted to the masonry wall using two high strength rods, which through of steel plates pulled the wall from its exterior face. On the reaction side, the force generated by the hydraulic jack reacted against Beam B, which transmitted the load to the upper and lower RC beams, and floor system. A scheme of the test rationale is shown in Figure 4.3.

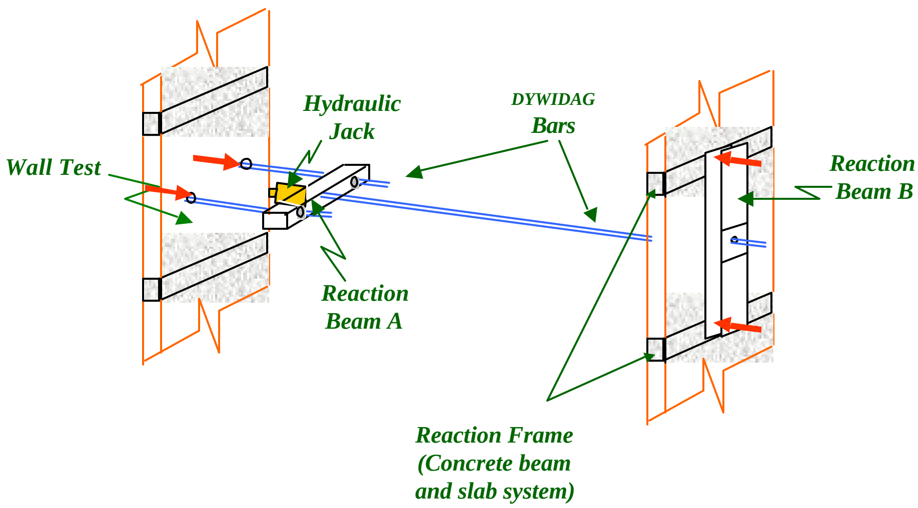

Figure 4.3. Out-of-Plane Test Rationale

Beam A was supported by a wooden panel resting on concrete blocks. Thin plates, which were greased, were placed between Beam A and the panel to reduce the friction restraint and provide smooth action (see Figure 4.4).

Figure 4.4. Beam A and Hydraulic Jack

Beam B was erected into place using an electric hoist located at the roof level (see Figures 4.5 (a) and 4.5 (b)). The hoist was restrained by a steel frame located on the roof of the building (see Figure 4.5). In this manner Beam B could be raised or lowered, depending on what wall was being tested.

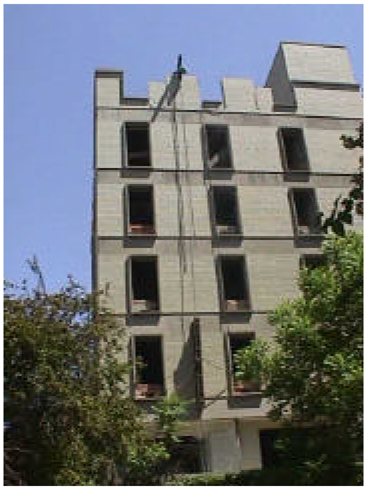

(a) Beam B hanging from hoist

(b) Beam B

Figure 4.5. Reaction System

Figure 4.6. Hoist and Metallic Frame

4.1.3. Test Procedure. The test setup was designed to load the URM walls with two concentrated loads, and measure deflections, strains and rotations due to these loads. As it will be discussed in Section 5, the top and bottom beams provided some fixity to the walls. The test conditions were like of those of walls away from corners, since both vertical edges were free.

The load was applied in cycles of loading and unloading. Each URM wall was loaded to 10 kips and then unloaded prior to continuing with the test. This procedure allowed checking the instrumentation and reacting systems. The walls were loaded in increments of 10 kips, and unloaded to 5 kips. The data obtained from a 200 kip load cell, Linear Variable Transducer (LVDTs), strain gages, and inclinometers were collected by a data acquisition system at a frequency of one point per second (see Figure 4.8). For the tests carried out in this experimental program eight LVDTs were used. LVDTs 1 to 5 intended to record out-of-plane deflections along the wall height. LVDTs 1 and 5 took into account the wall movement in the boundaries. LVDT 3 recorded midheight deflection, LVDT 6 monitored any movement in the upper RC beam, and LVDTs 7 and 8 intended to register the deflections along the wall length with the purpose of observing two-way action, if that was the case. Also five channels to record strains were employed, the strain gages were placed on the fibers or rods as shown in Figure 4.7. Three inclinometers were used to record rotations in the upper and lower borders, as well as in one of the free edges.

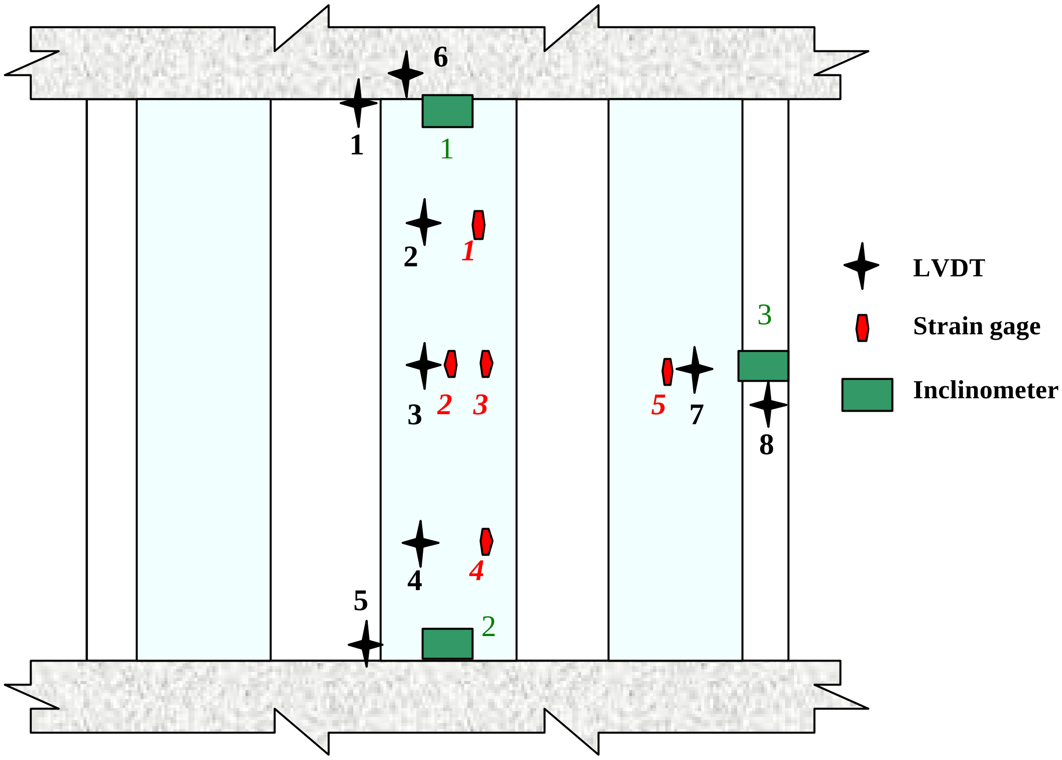

Figure 4.7. Test Instrumentation

4.2. IN-PLANE WALLS EXPERIMENTAL PROGRAM

4.2.1. Test Specimens. Four multiwythe reinforced masonry walls built using clay units were tested as part of this experimental program. The testing dimensions were 5 x 5 ft for three of these specimens (Walls 1, 2 and 3). A fourth specimen (Wall 4) of 7 x 5 ft. with an opening of 2 x 2 ft., was also evaluated. The overall thickness of the walls was 12.5 in.

The multiwythe walls were built with cored bricks with the following physical dimensions, 3.75 in. wide, 2.25 in. high and 8 in. long, the units had three cores of 1.5 in diameter. Details of the wall bond pattern are illustrated in Figure 4.8. The walls were reinforced with #3 bars, horizontally and vertically, which were placed in the bed joints and in the joint between wythes. The yielding strength of the reinforcement was 50 ksi Figure 4.9 illustrates a detail of the steel distribution.

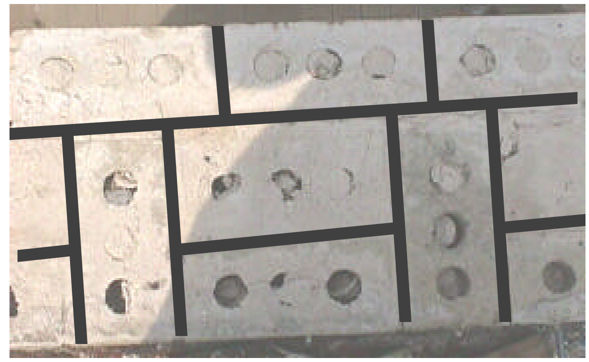

(a) Vertical Section (b) Horizontal Section

Figure 4.8. Cross Section of In-Plane Walls

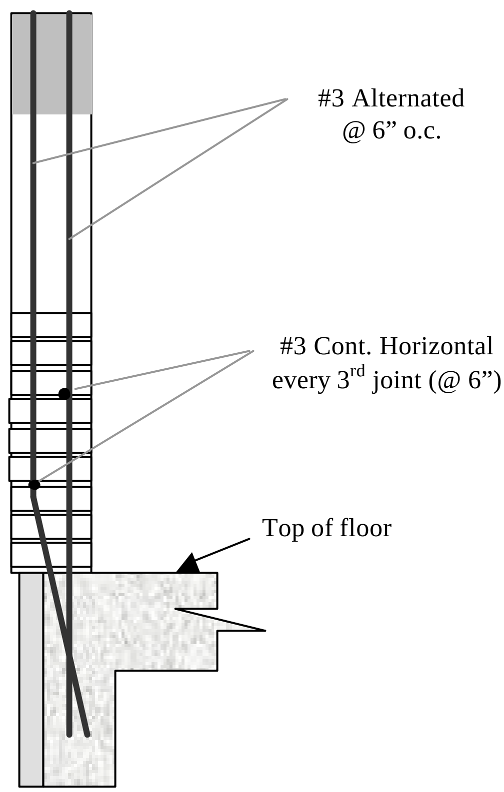

Figure 4.9. Steel Distribution for in-plane walls

Wall 1 was selected as a control specimen. The remaining three specimens were strengthened with GFRP sheets and rods. Wall 2 was strengthened with three 10-in. wide

GFRP strips vertically oriented and six #3 GFRP spaced at 10 inches horizontally oriented, as illustrated in Figure B.1 (Appendix B).

The strengthening scheme for Wall 3 was similar to that of Wall 2 with regard to the FRP sheets. Ten #3 GFRP rods, two by slot, were confined in 18 in. at each wall toe, their length was 36 in., details of the reinforcement are shown in Figure B.2 (Appendix B). The additional reinforcement had the purpose of increasing the flexural capacity and changing the mode of failure to a shear controlled to fully realize the effect of the horizontal sheets.

Wall 4 had a 2 x 2 ft. opening with out to out dimensions of 7 ft. long by 5 ft. high. A scheme of the strengthening scheme is illustrated in Figure B.3 (Appendix B). The test specimen was strengthened with four 8-in. wide GFRP strips vertically oriented and four 8-in. wide GFRP strips horizontally oriented. The strengthening in the toe regions was similar to that of Wall 3.

4.2.2. Test Setup. The masonry walls were loaded in-plane as cantilever walls, with free rotation at the top and fixed rotation at the base. The loads were generated by the alternated use of two 200 kip hydraulic jacks, which were produced by means of a hydraulic pump. Thus, two walls could be tested in cycles at the same time. A positive cycle was defined when by using Jack 1 the walls had an inward displacement (see Figure 4.10 (a)). The walls reacted against each other by means of two steel beams fabricated from C10x20 and two high strength rods. The in-plane forces were transmitted to the walls by 10x12-in. bearing plates, which had a steel rod to simulate a hinge connection. A negative cycle was defined when the load was applied by using Jack 2, which generated an outward displacement as illustrated in Figure 4.10 (b). The loads were transmitted to the walls by using similar plates to the aforementioned ones. Once the weaker wall had failed, after two or three positive and negative cycles, the remaining wall was loaded to failure, using Jack 1, by reacting against a contiguous stiffer wall as illustrated in Figure 4.10 (c).

The hydraulic jacks rested on a pile of concrete blocks and wood. Greased thin plates were placed underneath the jacks to reduce the friction restraint and provide smooth action. An overall view of the in-plane test setup is shown in Figure 4.11.

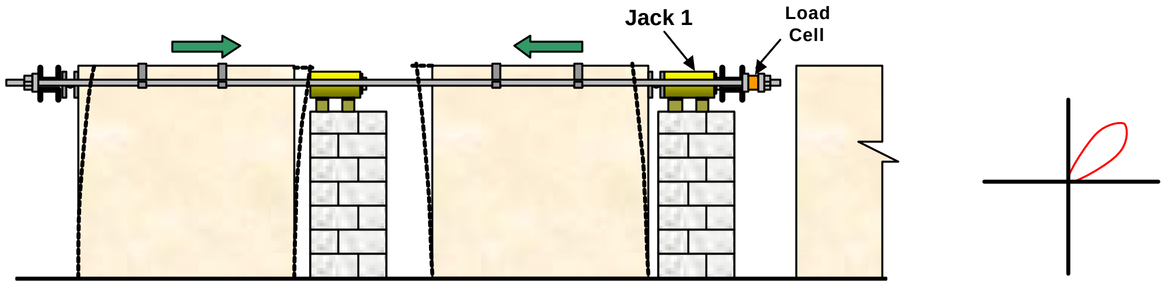

(a) Positive Cycle

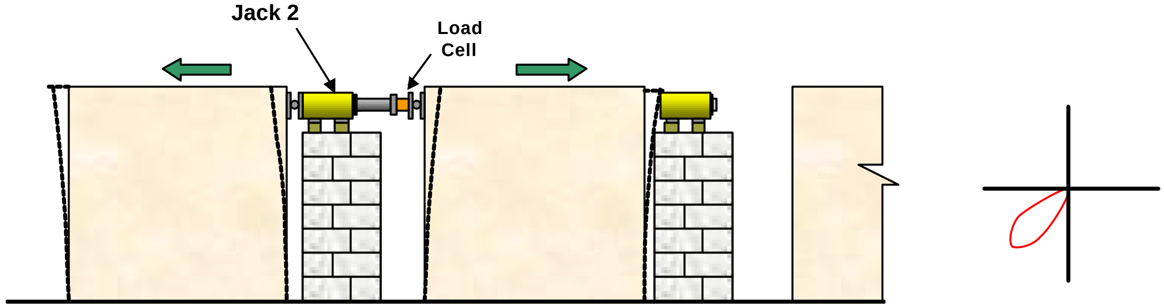

(b) Negative Cycle

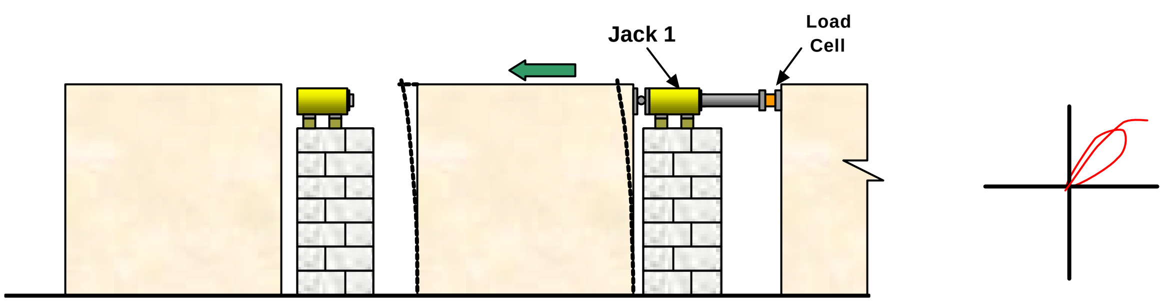

(c) Failure Cycle

Figure 4.10. In Plane Test Rationale

Figure 4.11. In-Plane Test Setup.

4.2.3. Test Procedure. A concentrated load was applied to the top of the walls. By means of LVDTs horizontal displacements were measured deflections due to the applied load. The load was applied in cycles of loading and unloading. The walls were loaded in increments of 5 kips. The data was collected by a data acquisition system at a frequency of one point per second similar to that used for out-of-plane testing. Three LVDTs were used to monitor in-plane movement in each wall. The first one was placed at the top to record the top displacement. The second one recorded displacements at the mid-height. Finally, the third one was placed near to the floor to detect any sliding of the wall, if that was the case.

5. TEST RESULTS

5.1. OUT-OF-PLANE TESTING

Results of the Out-of-Plane Testing including Load vs. Rotation at the Boundaries, Load vs. Mid-height Deflection, and Height vs. Deflection Curves are illustrated in Appendix C.

5.1.1. Results and Discussion

Wall 1

This wall was tested as a control specimen to determine the load-carrying capacity with the inclusion of the cementitious plaster. At 12 kips a first major horizontal crack was visible at mid-height, along the full bed joint (see Figure 5.1). At an applied load of 26 kips a second horizontal crack is formed, measured at a quarter height from the top of the wall. The peak load was reached at 30 kips for a mid-height deflection of 0.16 in as can be observed in Figure 5.2. The final failure is produced by a shear-compression combination effect, which ended with the fracture of the tiles placed at the bottom region of the wall. At the final stage part of the plaster, located at the bottom region of the wall is delaminated. It is important to highlight that in this specimen as well as in the remaining ones, no damage was observed on the exterior face of the veneer wall.

Figure 5.1. Horizontal crack in Wall 1

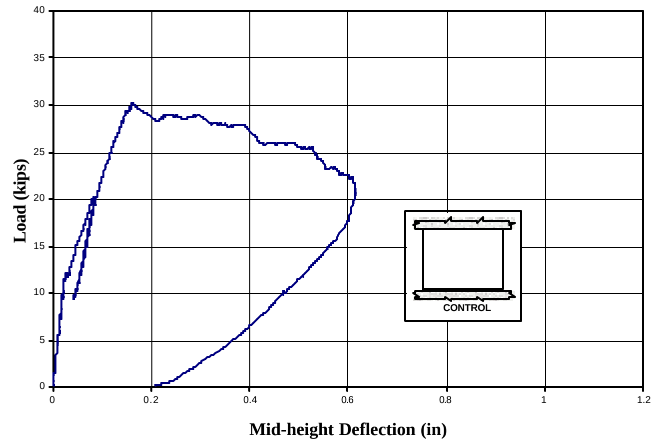

Figure 5.2. Load vs. Mid-height Deflection Curve – Wall 1

Wall 2

This wall was also tested as control specimen; however, in this case the cementitious plaster was removed from its surface with the objective of observing its influence on the overall wall behavior. The first visible crack was observed at a load of 10 kips, running above the central brick course, along the bed joint. The peak load was reached at 24 kips for a mid-height deflection of 0.16 in., the failure, similar to that observed in Wall 1, was caused by a shear-compression combination effect at the upper region of the wall. Once its peak was reached the load decreased to 20 kips and only the deflection increased. In comparison to Wall 1, this wall was less stiff, and it had quasi-elastic behavior up to failure, and can be observed from Figure 5.3.

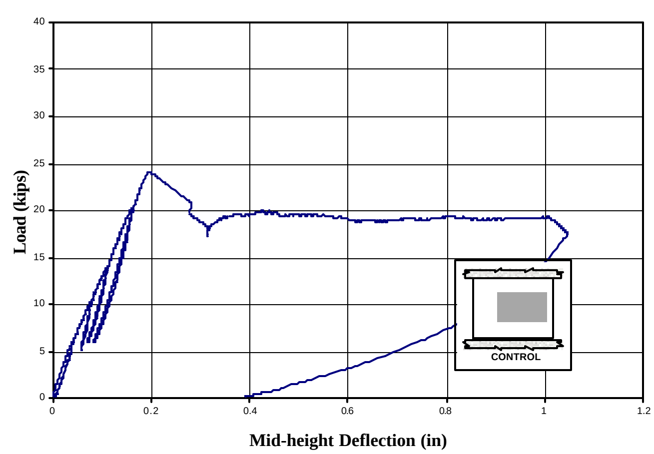

Figure 5.3. Load vs. Mid-height Deflection Curve – Wall 2

Wall 3

This wall was strengthened with three strips 20 in. wide of GFRP sheets. The first visible crack was observed at a load of 20 kips; at this stage the stiffness is slightly reduced. Two horizontal cracks are observed above the mid-height course. As shown in Figure 5.4, the wall failed at a load of 29 kips with a mid-height deflection of 0.1 in. at that stage. Delamination of the plaster at the lower area of the wall could be observed due to the loss of bonding between the plaster and the adjacent bricks and tiles, which were fractured by a shear-compression combination effect. In comparison with Wall 1, the presence of glass fibers delayed the first cracking, also, the crack width was thinner.

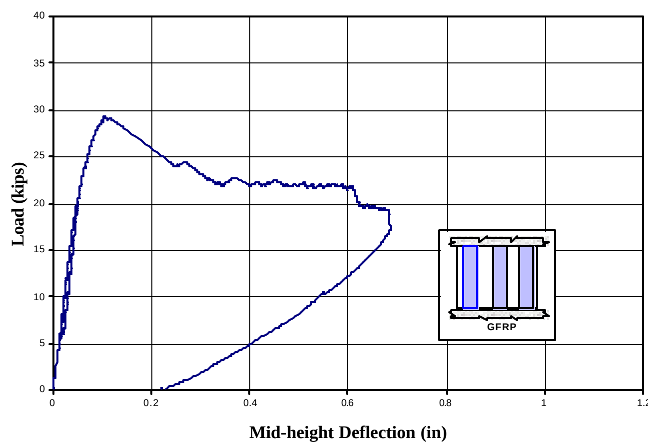

Figure 5.4. Load vs. Mid-height Deflection Curve – Wall 3

Wall 4

This wall had a similar strengthening scheme to Wall 3. The significant difference was that the glass fibers were applied directly on the masonry, meaning the plaster was previously removed. It was observed that the FRP reinforcement performed in a better fashion than the previous wall due to this alteration in the FRP installation procedure. The failure was caused by fracture of the masonry units located at the to of the wall (see Figure 5.5). However, the fact that the FRP was attached to the masonry made possible to observe a behavior more ductile than that observed in the previous wall, as can be observed in Figure 5.6. The maximum load recorded was 34 kips with a corresponding mid-height deflection of 0.2 in.

Figure 5.5. Fracture of Tile Unit

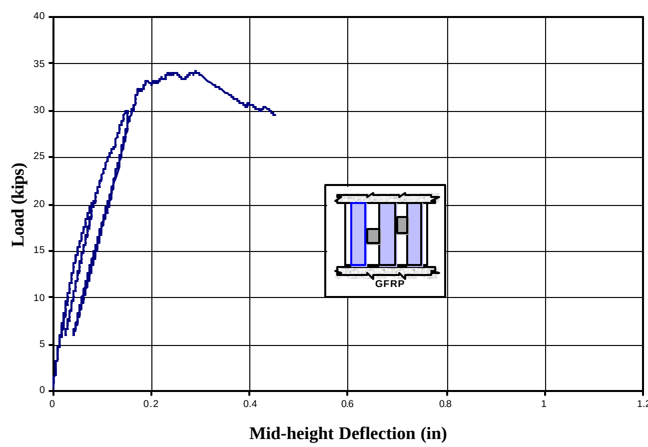

Figure 5.6. Load vs. Mid-height Deflection Curve – Wall 4

Wall 5

This wall was strengthened with half of the reinforcement used in Walls 3 and 4, meaning three strips 10 in. wide of GFRP fibers were attached to the wall surface. A horizontal crack above the mid-height course was observed at a load of 13 kips. Similarly to the previous walls, the failure was caused by a shear-compression combination effect at the lower region of the wall. The failure occurred at a load of 33 kips for a corresponding mid-height deflection of 0.12 in (see Figure 5.7). By comparing this wall to Wall 3, a larger presence of cracks spread for almost 50% of the area was observed (see Figure 5.8).

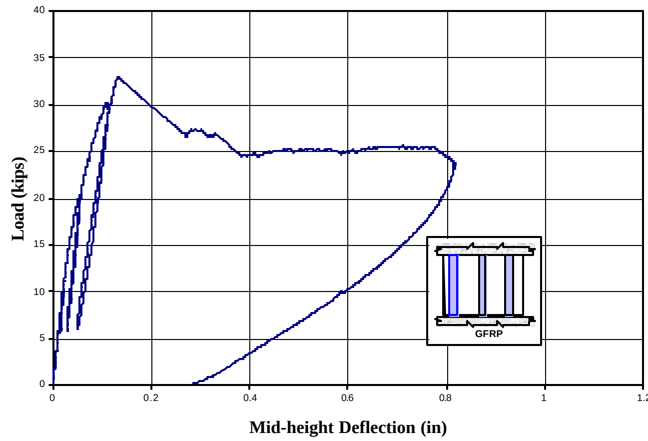

Figure 5.7. Load vs. Mid-height Deflection Curve – Wall 5

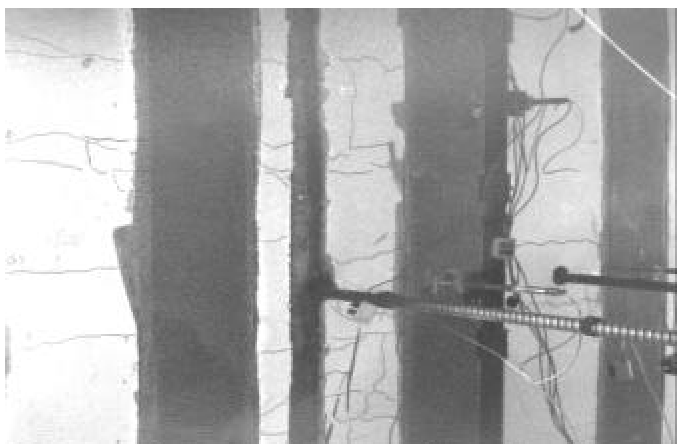

Figure 5.8. Cracking in Wall 5

Wall 6

This wall was strengthened with three strips 20 in. wide of CFRP sheets. A major horizontal crack was observed at a load of 24 kips, running along the bed joint located above the mid-height course. The maximum registered load was 30 kips, for 0.06 in mid-height deflection, as observed in Figure 5.9. The failure, brittle and without warning, was caused by a shear-compression combination effect, which fractured some tile units located at the bottom of the wall. As a consequence, with the deflection increasing the plaster layer delaminated from the adjacent tiles as can be observed in Figure 5.10. This wall showed an atypical behavior compared to the other walls. As can be observed in the corresponding Height vs. Displacement curve in Appendix 2, the upper region of the wall displaced in opposite direction to the applied load.

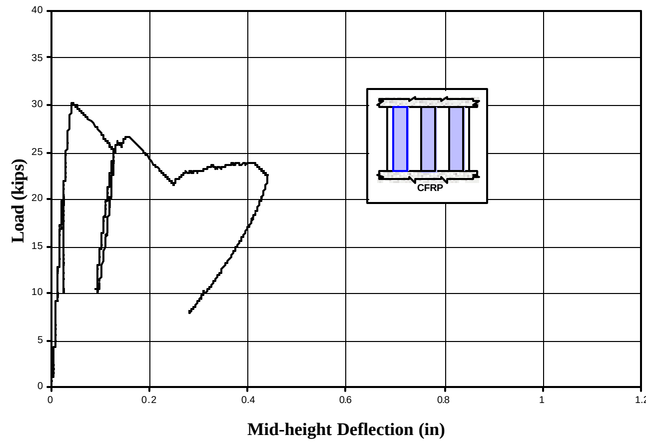

Figure 5.9. Load vs. Mid-height Deflection Curve – Wall 6

Figure 5.10. Fracture of units at the bottom of Wall 6

Wall 7

The strengthening geometry of this wall was similar to the previous wall, only that in this case AFRP sheets were used. This wall did not show large areas of cracking, only a major horizontal crack running along the mid-height was detected at a load of 24 kips. The peak load was 36 kips with a corresponding mid-height deflection of 0.12 in. (see Figure 5.11). Delamination of the plaster on the top region of the wall was observed as a consequence of the fracture of the tiles, as shown in Figure 5.12

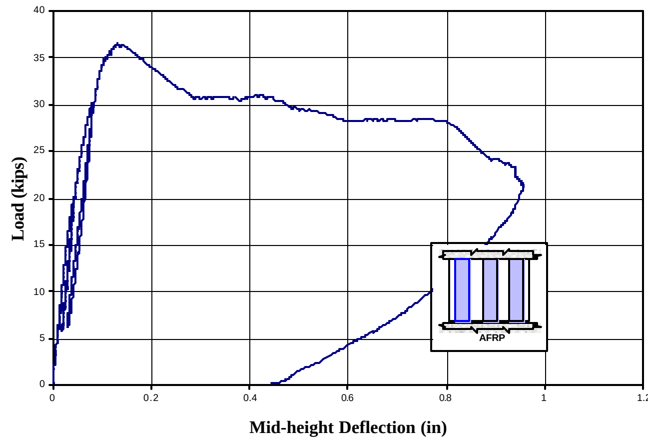

Figure 5.11. Load vs. Mid-height Deflection Curve – Wall 7

Figure 5.12. Plaster Delamination

Wall 8

The strengthening geometry of Walls 3 and 8 were similar. The only difference was the employment of glass rods in Wall 8 in order to give continuity to the GFRP sheets into the RC beams. Since the controlling factor was the fracture of the tiles located at the bottom region of the wall, the results were identical to those found in Wall 3. The peak load was 29 kips with 0.1 in mid-height deflection, as observed in Figure 5.13.

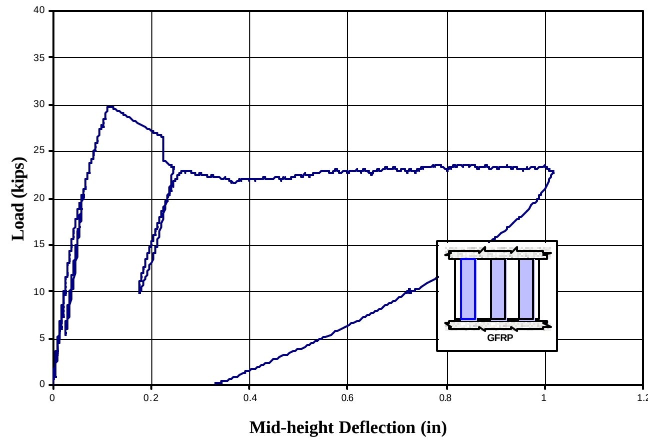

Figure 5.13. Load vs. Mid-height Deflection Curve – Wall 8

Wall 9

This wall was strengthened with eight #3 glass rods. The first visible crack was observed at 22 kips running along the upper joint of the mid-height course (see Figure 5.14). The wall failed at 24 kips for a mid-height displacement of 0.06 in (see Figure 5.15). The lower capacity may be caused by pre-existing cracking formed during the installation of the rods. The installation procedure weakened the by themselves already fragile clay tiles facilitating the failure. The failure was originated by a shear-compression combination effect, which fractured some tiles at the lower part of the wall.

Figure 5.14. Horizontal crack in Wall 9

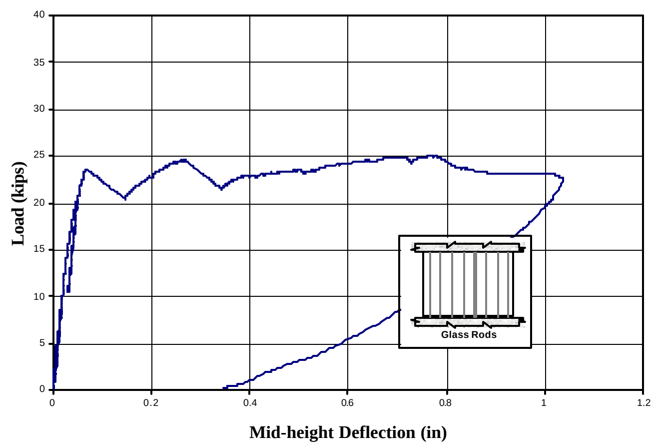

Figure 5.15. Load vs. Mid-height Deflection Curve – Wall 9

Wall 10

This specimen was also strengthened with eight #3 glass rods. As mentioned in Section 4, the near-surface-mounted rods were anchored to the upper and lower beams. The first visible crack, at mid-height course, was observed at 20 kips for a corresponding displacement of 0.09 in. As observed in Figure 5.16, the wall failed at 26 kips, in similar way to the previous one. The cause of the failure was also attributed to the presence of cracking prior to testing.

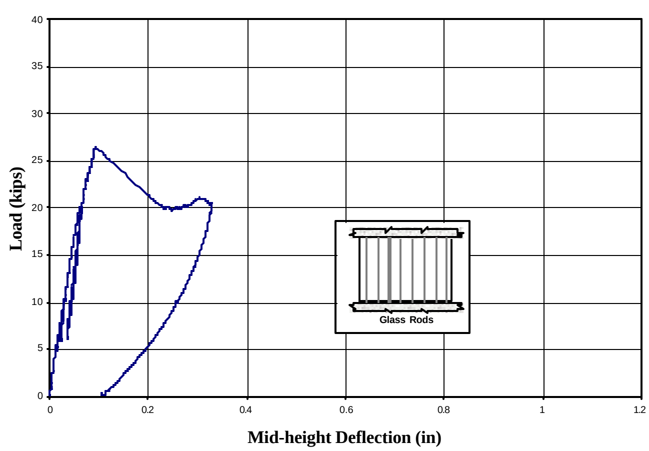

Figure 5.16. Load vs. Mid-height Deflection Curve – Wall 10

5.1.2. Comparisons. By observing Figure 5.17, Control Wall 1, with plaster, showed a capacity 25% larger than that found in Control Wall 2, without plaster. After reaching 12 kips, point where the first horizontal cracks occurred in Wall 1, a substantial difference in the stiffness *K* (*K a EI*) is observed. This difference is attributed to an increment in the overall moment of inertia of the wall due to the extra inch of the plaster thickness, and due to the different modulus of elasticity in the masonry and cementitious plaster. From the same figure it is observed that FRP sheets do not perform adequately when they are attached to the plaster surface, as can be concluded from the corresponding tests performed on Wall 1 and Wall 3, where no increment in capacity was registered. In contrast, when the FRP was attached directly on the masonry by removing the plaster, an increment of 40% in capacity was observed by comparing Wall 4 to the Control Wall 2.

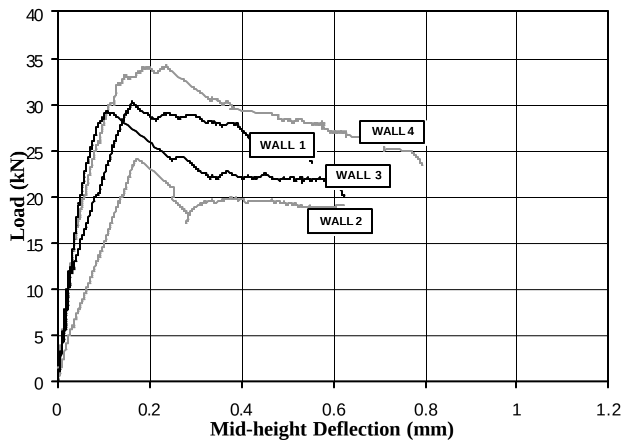

Figure 5.17. Behavior Comparison of Walls 1, 2, 3 and 4

The aforementioned increment in capacity is attributed to a better engagement of the FRP sheets to the surface when the out-of-plane bending increases. This can be corroborated from Figure 5.18, where up to a load of 20 kips the strains developed in the FRP sheets attached to Wall 4 doubled those of Wall 3.

From Figure 5.19, it is observed that Wall 3 and Wall 8 had the same behavior. The rods placed in Wall 8 did not have influence since the failure was controlled by a shear- compression effect, which fractured the tiles in the upper region of the wall. Also, it can be observed that Wall 5, with half amount of reinforcement respect to the other Walls, showed a slightly higher capacity.

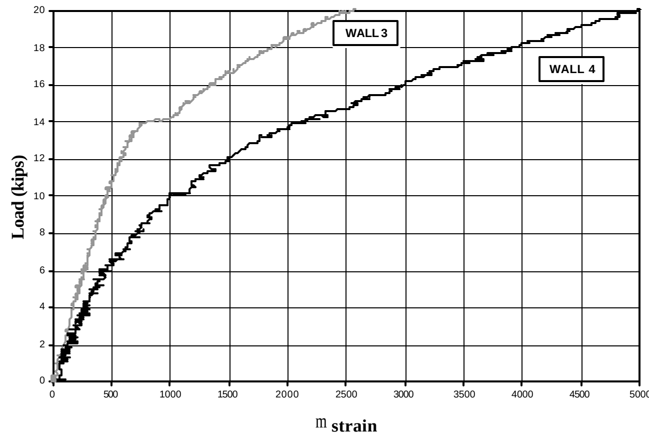

Figure 5.18. Strain Comparison for Walls 3 and 4

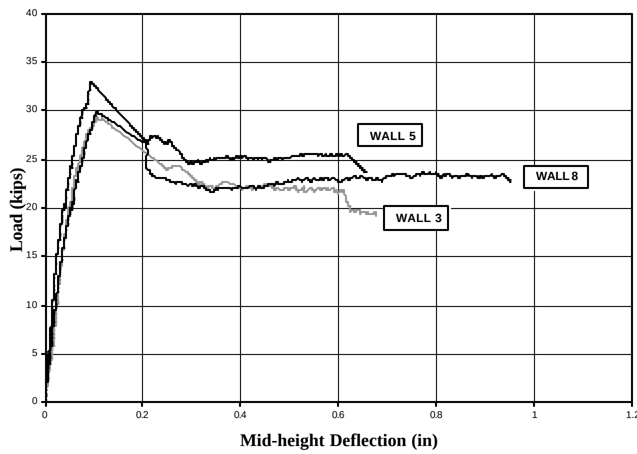

Figure 5.19. Behavior Comparison of Walls 3, 5 and 8

As observed in Figure 5.20, Wall 9 and Wall 10 showed lower capacities than the Control Wall 1, which may be attributed to a weakening of the masonry units during the installation of the rods. As it was mentioned in Section 3, FRP rods were mounted into slots grooved on the masonry surface using a grinder and chisel. This procedure may have pre-cracked the wall. The use of near-surface-mounted rods is attractive since the removal of plaster is not required; however, their installation should be limited to strengthening of walls built of solid brick units or grouted concrete walls.

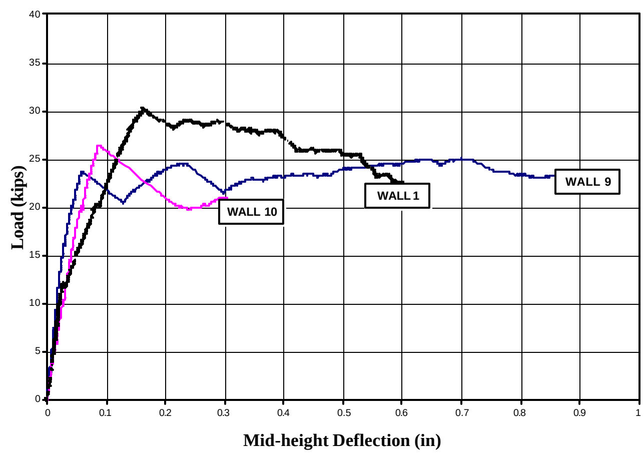

Figure 5.20. Behavior Comparison of Walls 9 and 10

In Figure 5.21 can be observed the increment of stiffness, from smaller to larger, when GFRP, AFRP and CFRP sheets were used. The higher capacity of Wall 7 compared to the other walls is not statistically significant since its value is within the variability of the capacity values and because the fracture of tiles is controlling its behavior. During the tests, it was observed that the employment of FRP sheets delayed the presence of the first visible cracks, and also, that the crack widths were reduced.

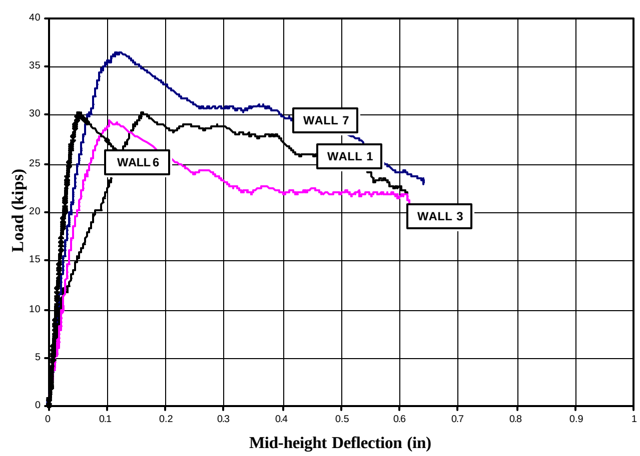

Figure 5.21. Behavior Comparison of Walls 1, 3, 6 and 7

The walls suffered more rotations in the zone where the main fracture occurred. Their values were small, averaging 0.25^{o}, they produced angular distortion, which is critical in a masonry unit composed of thin walls such as the case of the clay tiles. The angular distortion along with a shear-compression combination effect caused the fracture of the units located either at the top or bottom of the wall. Larger rotations were accompanied, most of the times, by larger displacements at that zone due to either starting of plaster delamination or spalling of the tile shell, which were caused by the fracture of the tiles. As example the Load vs. Rotation curve corresponding to Wall 7 is presented in Figure 5.22, in this case fracture of tiles was observed at the top of the wall.

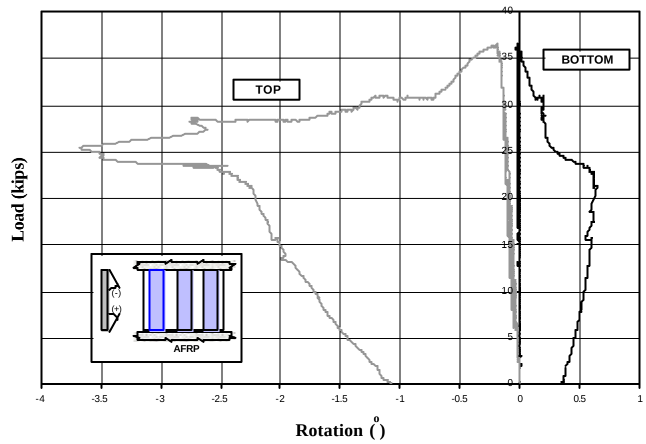

Figure 5.22. Rotations in Wall 7

5.1.3. Mechanism of Failure

The failure of the URM walls was caused by the fracture of the tile units placed on the uppermost or bottommost courses. The fracture of these tiles is caused by angular distortion due to out-of-plane rotation, and mainly by a force generated by a shear-compression combination effect. Flexural cracking occurs at the supports due to negative moments followed by cracking at mid-height due to positive moments, as a result a three-hinged arch is formed. When the deflection increases due to out-of-plane bending the wall is restrained against the supports, in this case the upper and lower beams. This action induces an in-plane compressive force (F_V in Figure 5.23), which accompanied by the shear force (F_H in Figure 5.23) in the support create a resultant force that causes the fracture of the tile (F_R in Figure 5.23). It is important to mention that normally the crushing is associated to the mortar joint; however, due to the brittle characteristics of the tile, the failure here was associated with the tiles. Once the fracture of the tiles was initiated, the adjacent plaster layer began to delaminate from the masonry surface. At this stage, since the FRP adhered to the plaster surface was not able of engaging the flexural cracks, the wall capacity degraded. In contrast where the externally bonded FRP strips were attached directly to the masonry, the failure was delayed because the FRP were able to engage the flexural cracks running through the bed joints. Consequently, the wall capacity was improved but the mechanism of failure did not change.

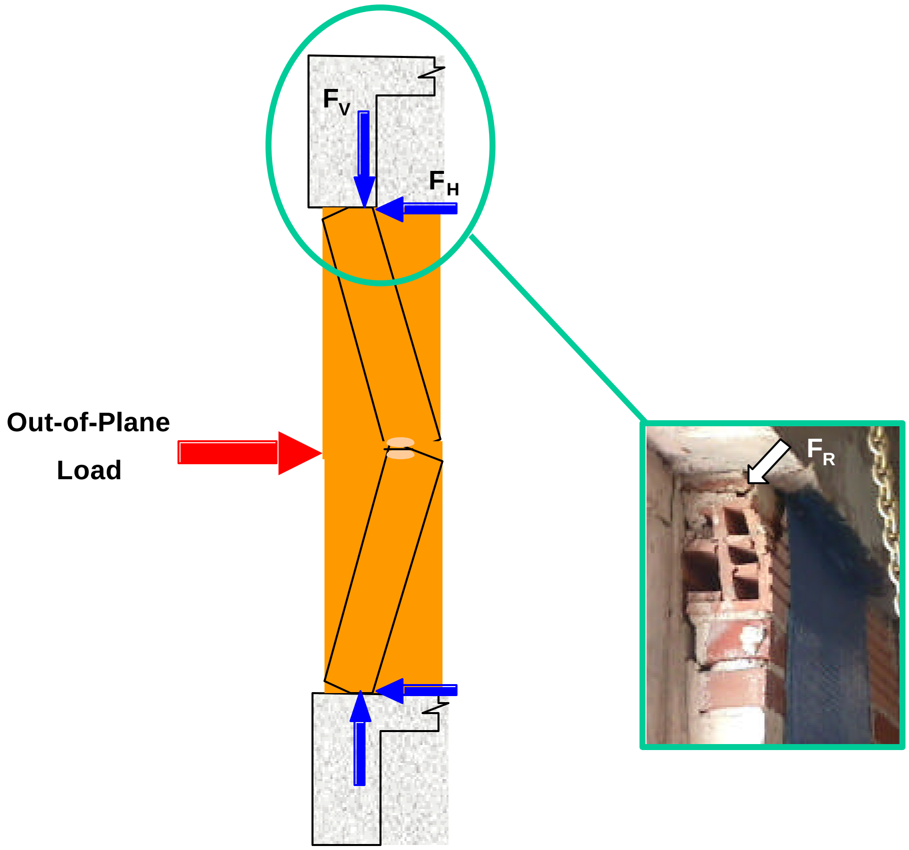

Figure 5.23. Out-of-Plane Mechanism of Failure

5.2. IN-PLANE TESTING

Due to the low load applied during the tests only two cycles were applied, an envelope of the load vs. top displacement curves is illustrated in Figure 5.24. This envelope includes the cycle where the failure occurred, either positive or negative cycle. The curves showing the positive and negative cycles, as defined in Section 4 (see Figure 4.11), are shown in Appendix D.

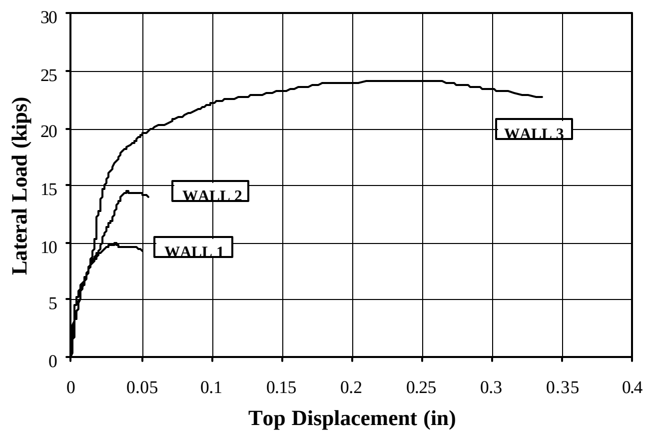

Figure 5.24. Lateral Load vs. Top Displacement – Walls 1, 2 and 3

Wall 1 was used as control specimen to determine the flexural capacity of the walls subjected to in-plane loading prior to being strengthened. A flexural crack was visible at the base of the wall for a load of 2 kips. A maximum force of 10 kips occurred for a displacement of about 0.3 in. The wall lost carrying capacity due to the crack growth. The crack length when the test was stopped covered approximately two-thirds of the base length (see Figure 5.25). Base sliding was not observed at this final stage. Compared to the expected moment capacity of 122.6 ft-kips, which is associated to an in-plane load of 22.3 kips, the wall exhibited a lower value. This can be attributed to a deficient anchorage of the vertical steel reinforcement, which could have been pulled out from the wall. As it was mentioned in Section 4, the steel reinforcement was placed in the space between the whytes, which was filled with mortar.

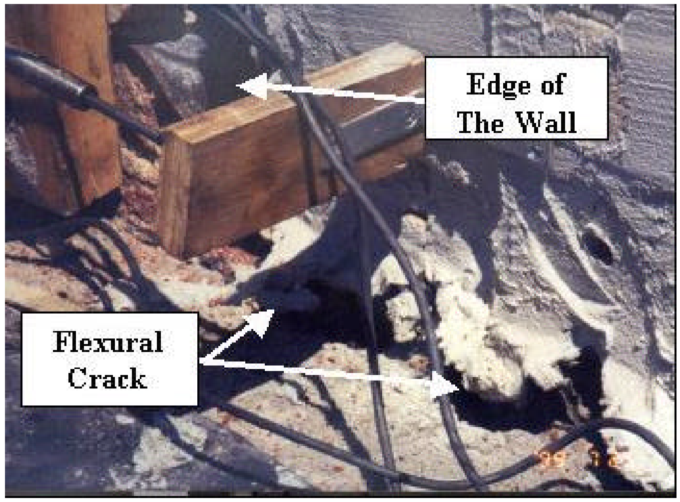

Figure 5.25. Flexural Crack at the bottom of Wall 1

Wall 2 was strengthened with GFRP sheets vertically oriented and GFRP rods horizontally oriented. Similarly to Wall 1, a flexural crack was observed at the base of the wall for a load of 3.5 kips. Flexural failure was observed at 14 kips for a displacement of 0.04 in. Owing to the fact that the GFRP sheets bridged some horizontal cracks (see Figure 5.26), close to the bottom of the wall, an increase of 40% in capacity was observed. However, the main crack, which caused the failure was observed at the bottom of the wall, in similar way as compared to Wall 1.

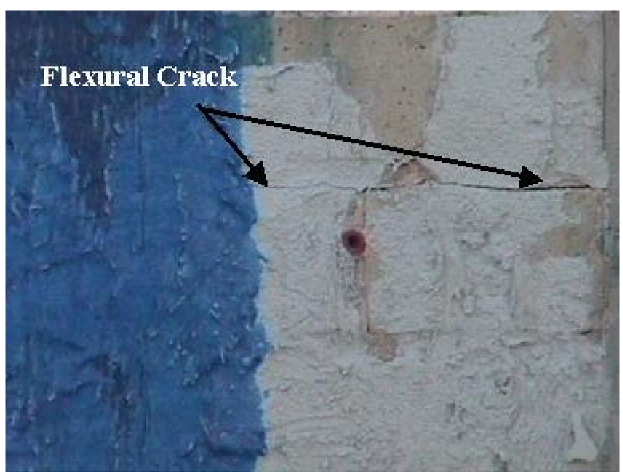

Figure 5.26. Flexural Crack in Wall 2

In order to increase the flexural capacity of the walls and induce a shear failure, near-surface-mounted GFRP rods were installed in the toes of the Walls 3 and 4, as previously described in Section 4. The strengthening scheme of Wall 3 was similar to that of Wall 3. A crack running along the base of the wall was visible at a load of 5 kips. A flexural failure was observed for a maximum load of 24 kips with a corresponding displacement of about 0.18 in. After reaching a displacement of about 0.3 in., significant load degradation was observed. The opening of the horizontal crack in the strengthened side was controlled by means of the GFRP rods. However, the eccentric tensile forces in the GFRP rods caused by the strengthening of only one face of the wall, made the wall tilt, which forced to stop the test. In Figure 5.24, by comparing Wall 3 to Wall 2, without near-surface-mounted rods in the toes regions, the increment in capacity was about 70%.

Since the steel reinforcement was pulled out, the concept of ductility defined as the ratio between the deflection at the ultimate state of failure and the deflection at the yielding of steel can not be applied. However, in Wall 3, due to the contribution of the GFRP rods in the toes, a notable increase in pseudo-ductility was attained, as illustrated in Figure 5.24.

Wall 4 was also strengthened with GFRP sheets and near surface mounted GFRP rods. The purpose of testing this wall was to observe the influence of openings in the wall behavior. Two main flexural cracks were observed; one along the base of the wall, and the other at a height of 2.5 ft., at the cut point of the GFRP rods. The latter flexural crack ended up in the border of the opening, as observed in Figure 5.27.

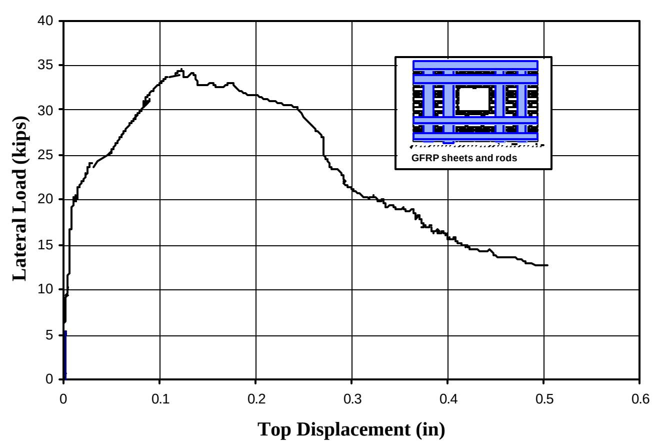

Figure 5.27. Lateral Load vs. Top Displacement – Wall 4

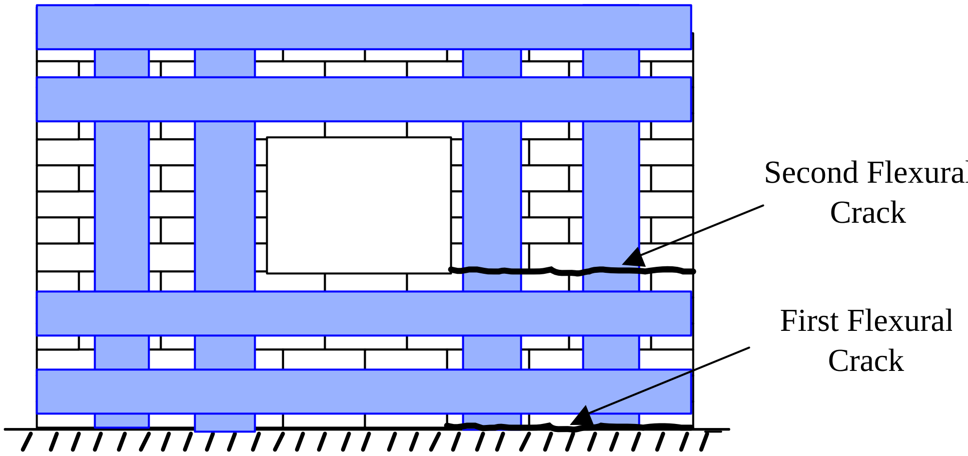

Figure 5.28. Cracking Pattern in Wall 4.

6. CONCLUSIONS

6.1. OUT-OF-PLANE PROGRAM

The singular opportunity of testing URM walls at the Malcolm Bliss Hospital allowed to identify a mechanism of failure that is not commonly observed in tests performed in a laboratory environment, where simply supported boundary conditions are considered. This mechanism of failure is not usually considered in the quantification of upgraded wall capacities, which can dangerously lead to overestimate the wall response during a seismic event.

In addition, it was observed that the wall where the FRP was applied on the tile surface, after the removal of plaster, exhibited a better performance than its counterpart, strengthened without the removal of plaster. The increase in capacity was about 17 % compared to the wall strengthened with the presence of plaster, and 45 % compared to the control wall without plaster.

The use of near-surface-mounted rods is attractive since the removal of plaster is not required; however, due to the technique used for their installation, which can create local damage in the masonry, their use should be limited for strengthening of walls built of solid brick units or grouted concrete walls.

In order to fully realize the benefits of the use of FRP composites, the strengthening techniques should address the boundary components. For the test walls investigated herein, one strengthening alternative could be to grout the tiles to “push” the failure mode into the FRP rather than the boundary conditions.

Finally, an analytical model is presented for determining the transverse load that both unreinforced and externally strengthened infill walls can resist.

6.2. IN-PLANE PROGRAM

For the shear strengthening, adequate performance of the FRP relied on the distribution and anchorage of the existing steel reinforcement. Details including the size spacing, and the development of reinforcing was assumed based on original construction documents. Due to pullout of the vertical reinforcement and the absence of some of the horizontal and vertical steel reinforcement, the full benefits of the FRP strengthening were not realized. It is important to note that when the internal reinforcement is not an issue in the strengthening strategy, a good performance of the strengthening design rests on building plans, which are assumed to have been materialized following pertinent construction standards.

In spite of the difficulties found during the execution of this experimental program, the test results demonstrated that, under in-plane loading, the use of near-surface-mounted rods confined to the toe region of the walls were able to provide a ductile behavior for masonry walls. Also, a great increment in the flexural capacity of the walls was observed.

APPENDIX A

STRENGTHENING SCHEMES FOR

OUT-OF-PLANE PROGRAM

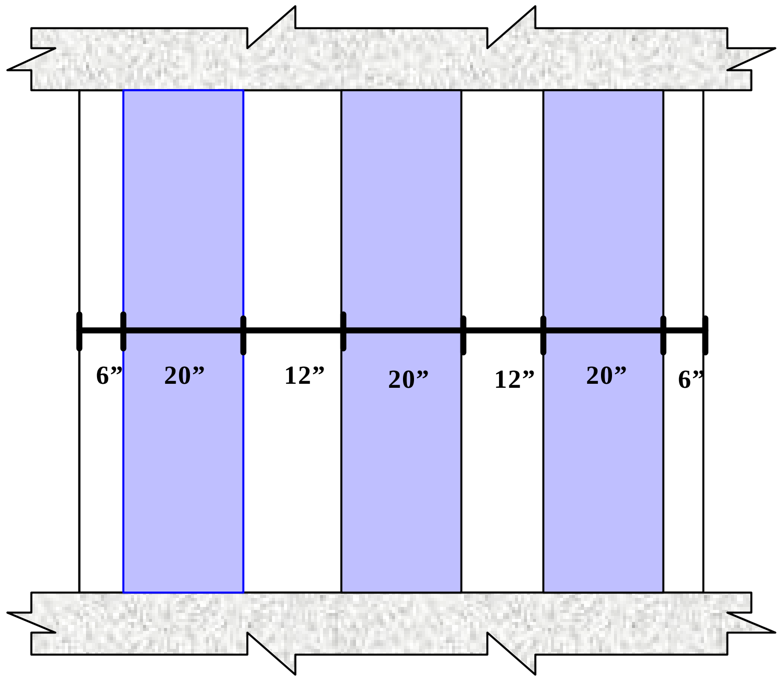

Figure A.1. Out-of-Plane Strengthening Scheme – Walls 3, 4, 6 and 7

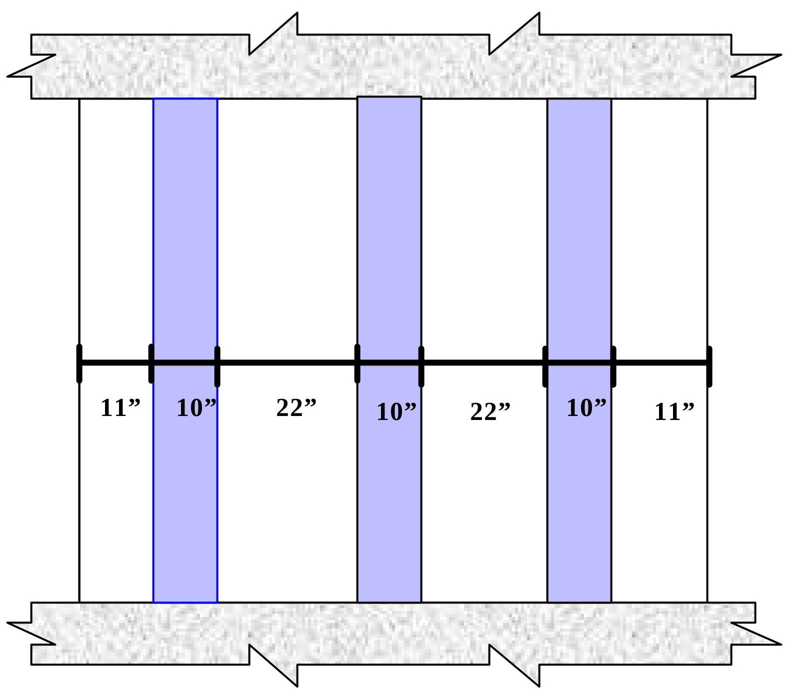

Figure A.2. Out-of-Plane Strengthening Scheme – Walls 5

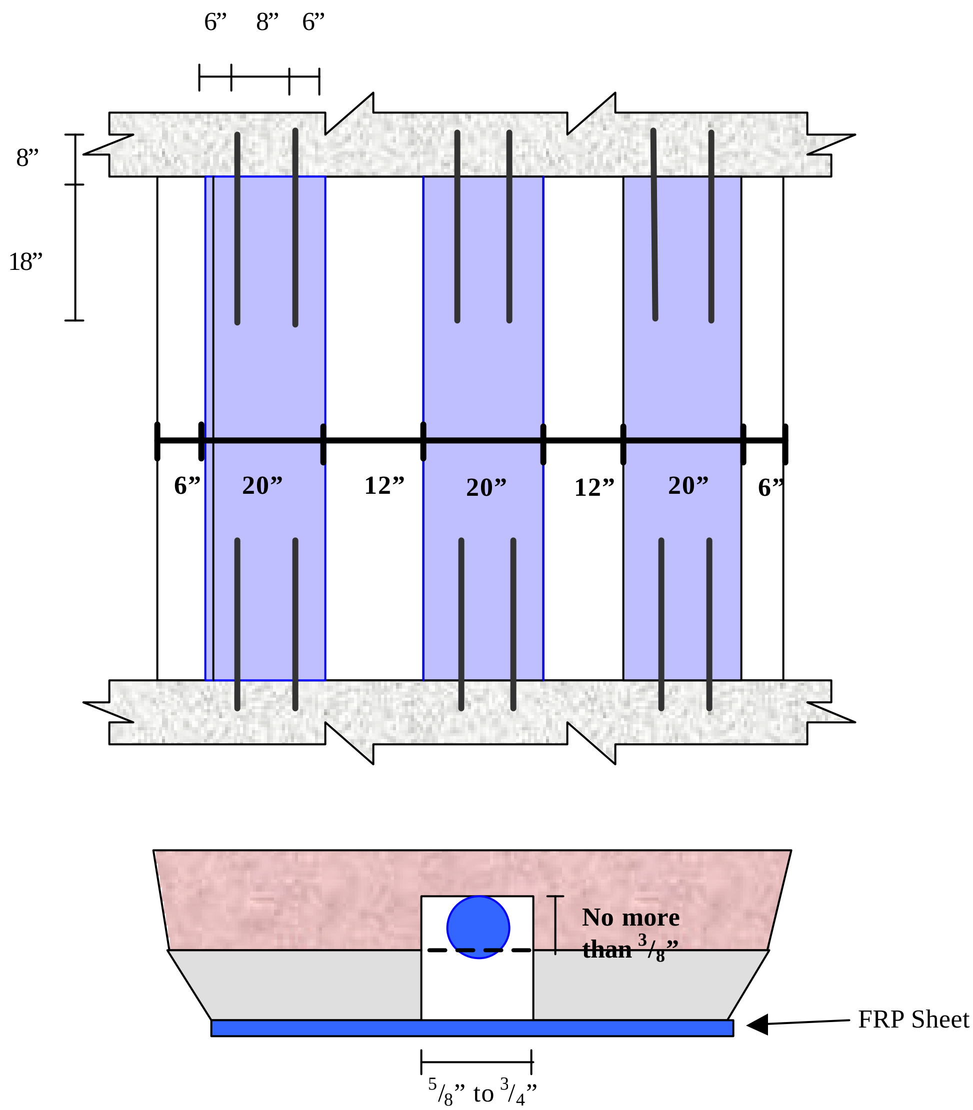

Figure A.3. Out-of-Plane Strengthening Scheme – Walls 8

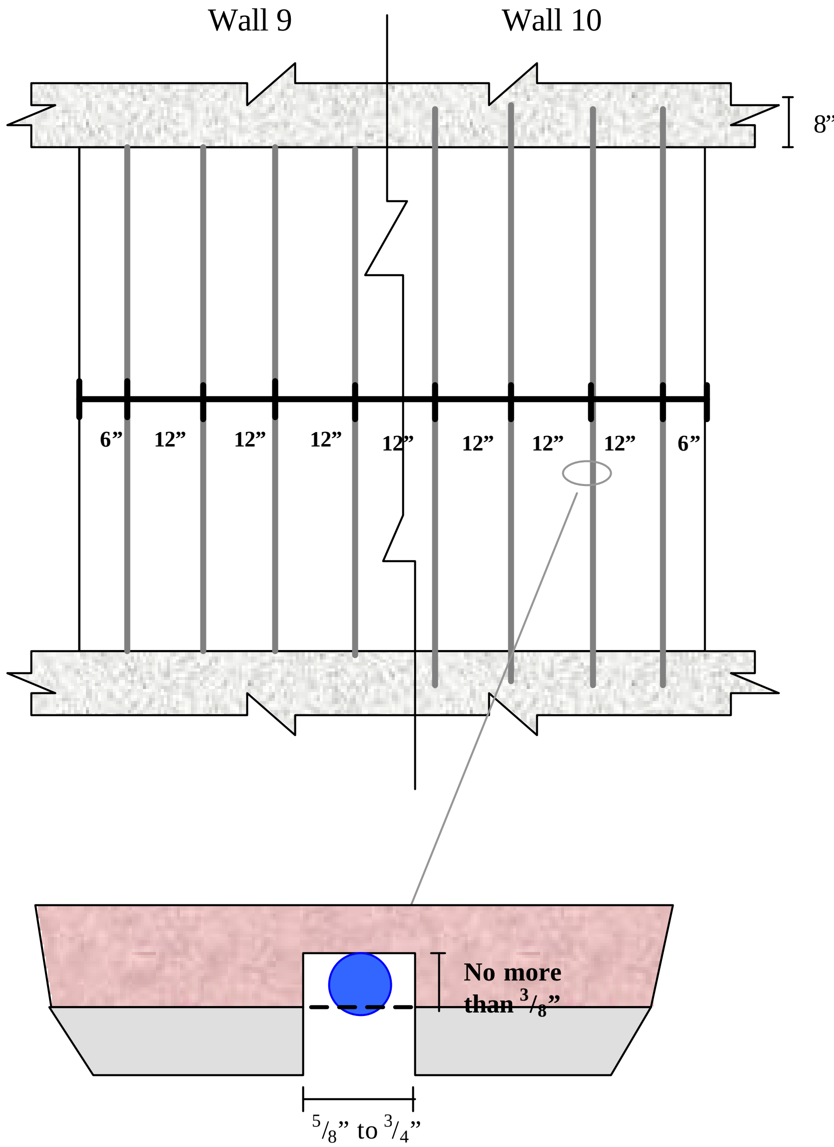

Figure A.4. Out-of-Plane Strengthening Scheme – Walls 9 and 10

APPENDIX B

STRENGTHENING SCHEMES FOR

IN-PLANE PROGRAM

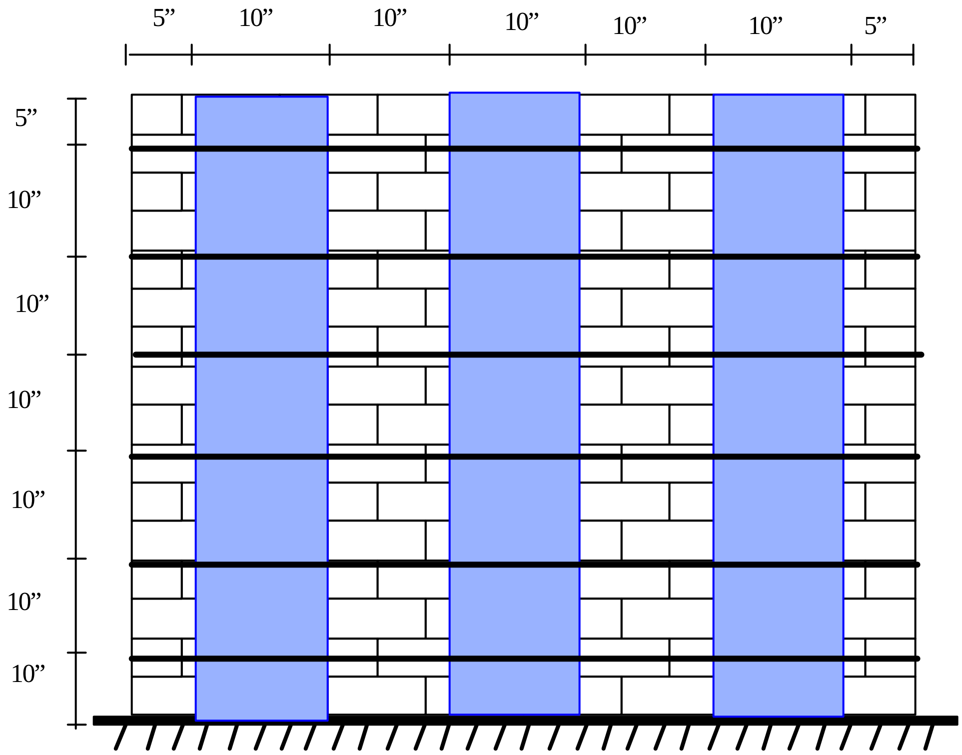

Figure B.1. In-Plane Strengthening Scheme – Walls 2 and 3

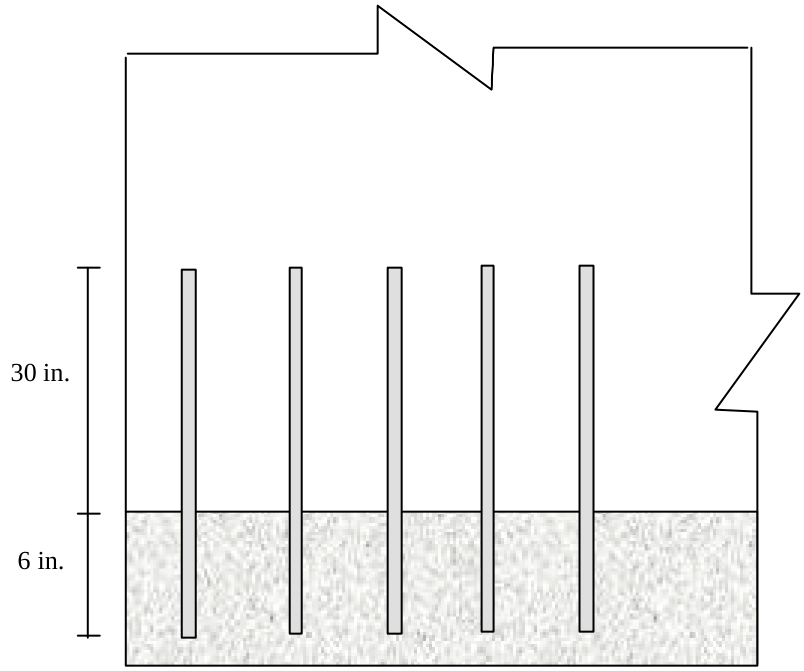

(a) Elevation view

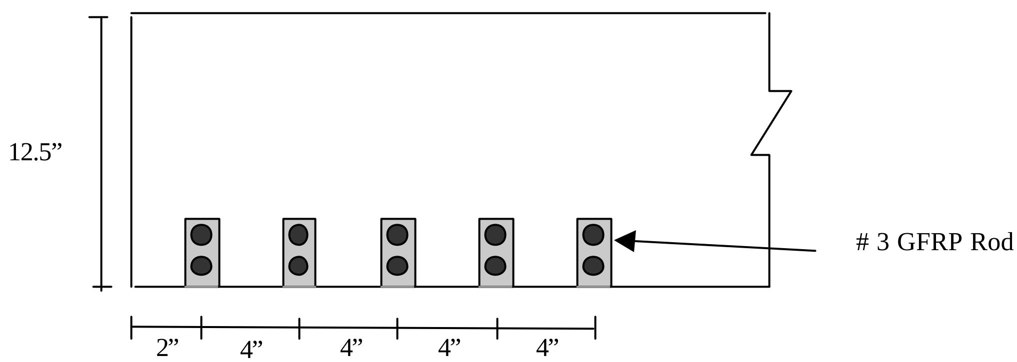

(b) Plan view

Figure B.2. Detail of GFRP Rods Reinforcement

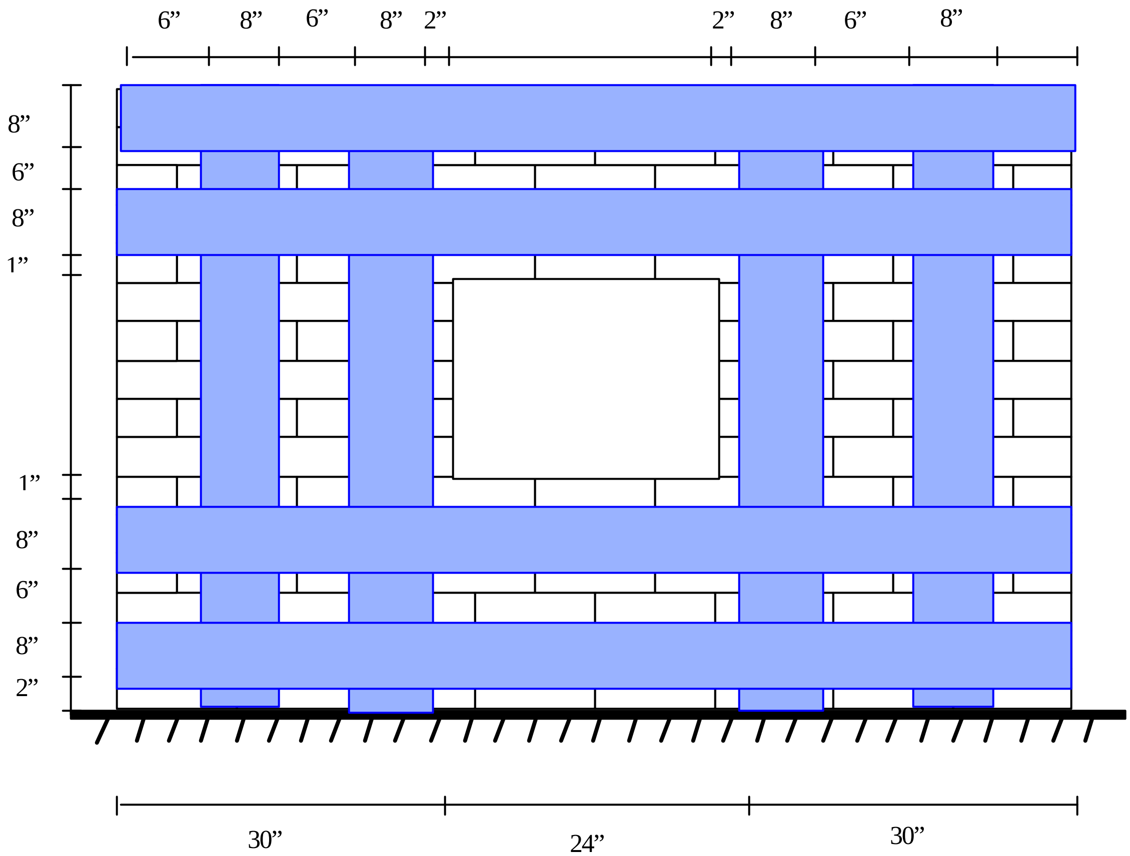

Figure B.3. In-Plane Strengthening Scheme – Wall 4

APPENDIX C
OUT-OF-PLANE TEST RESULTS

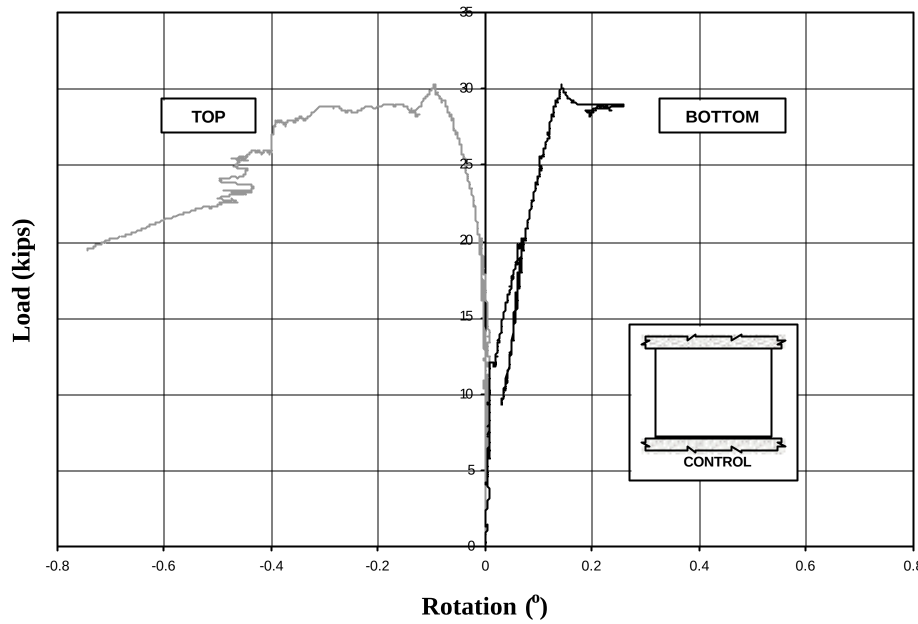

Figure C.1. Load vs. Rotation – Wall 1

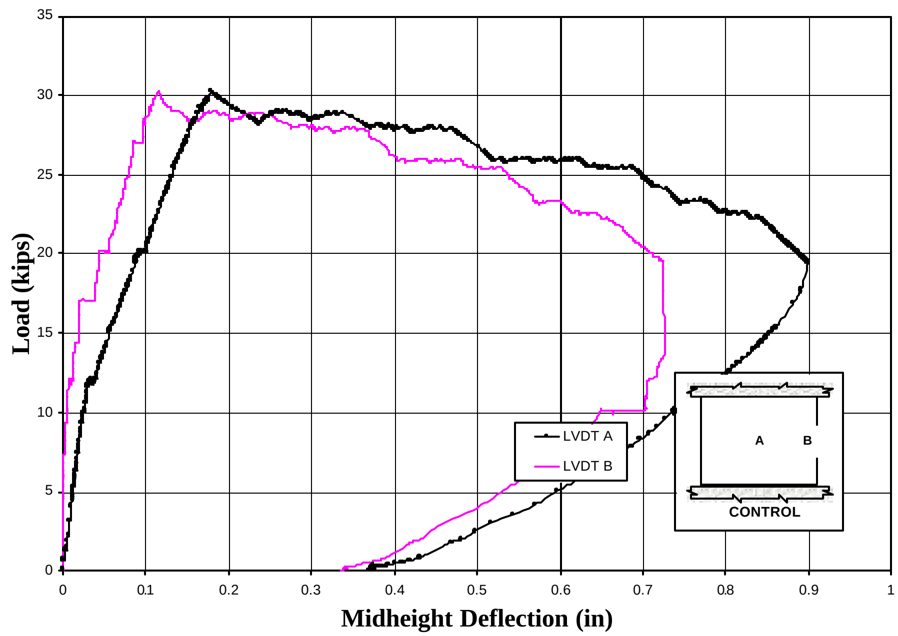

Figure C.2. Two- way action –Wall 1

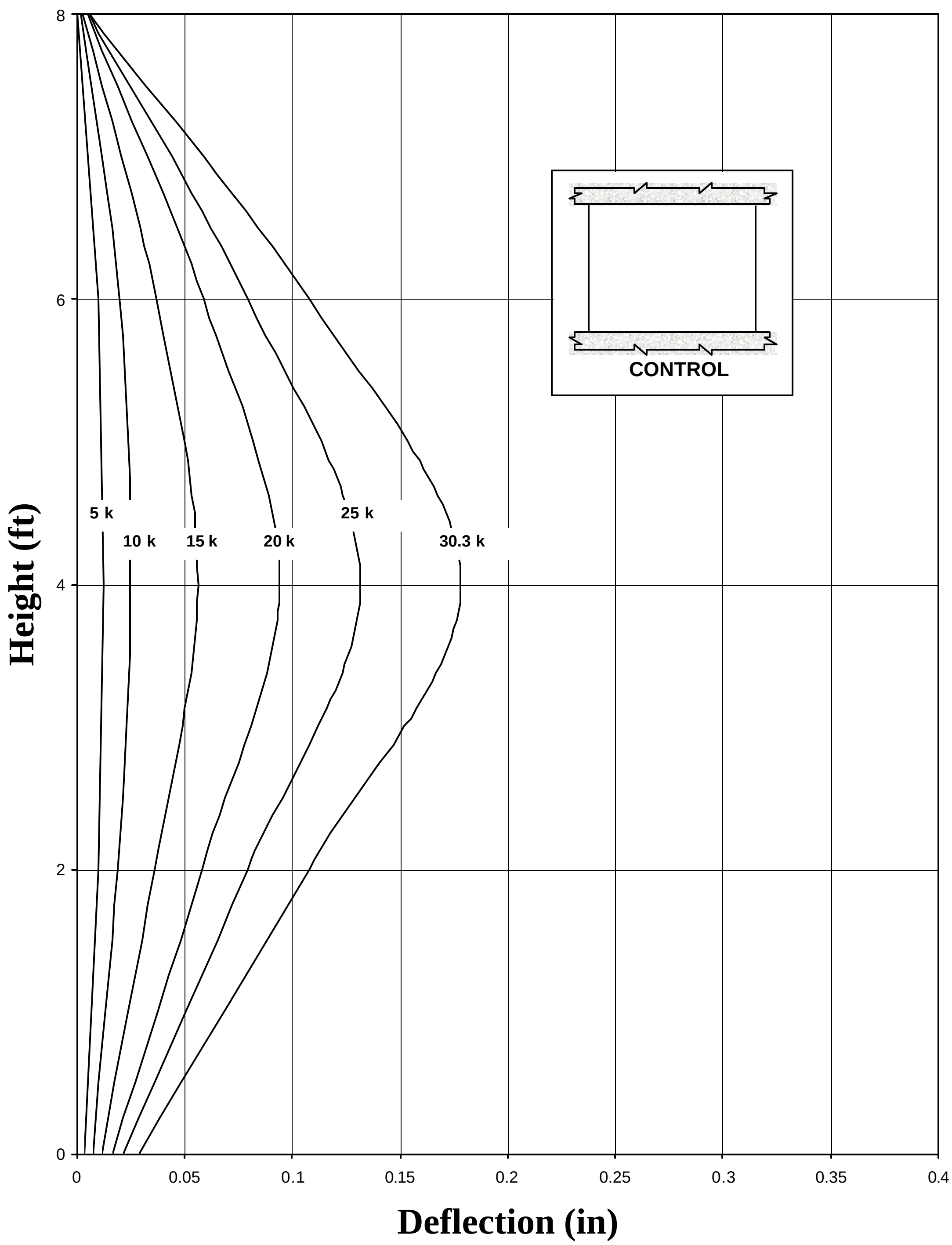

Figure C.3. Height vs. Deflection – Wall 1

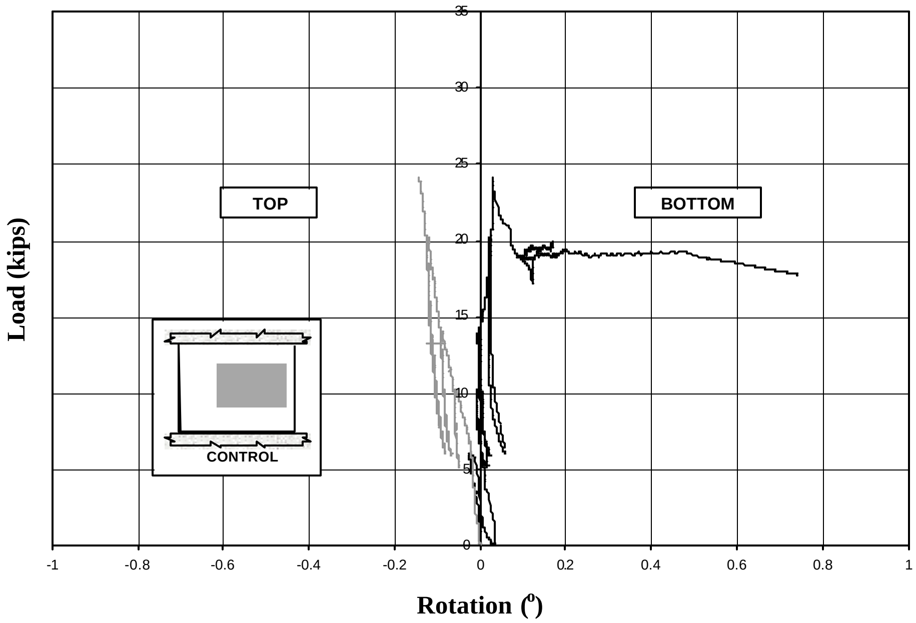

Figure C.4. Load vs. Rotation – Wall 2

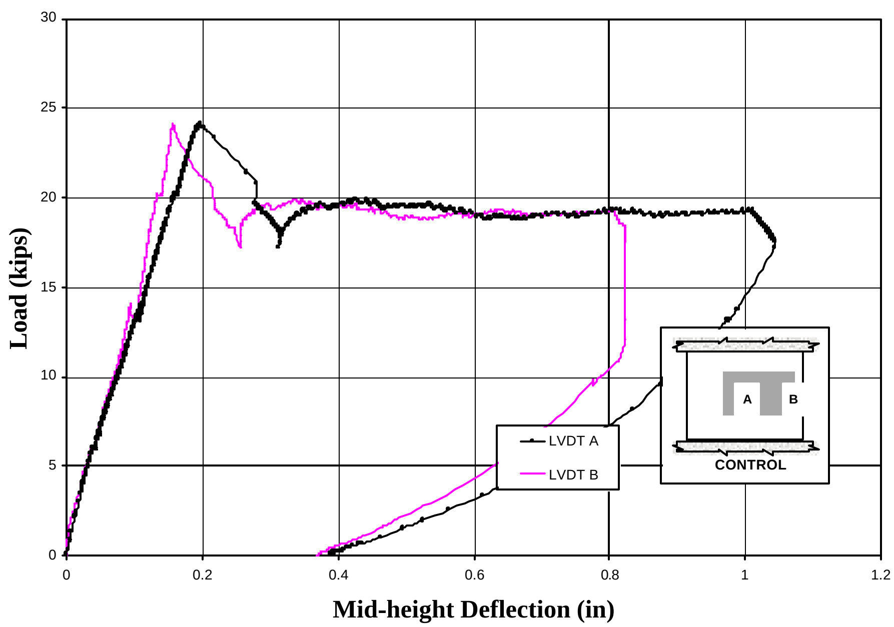

Figure C.5. Two- way action –Wall 2

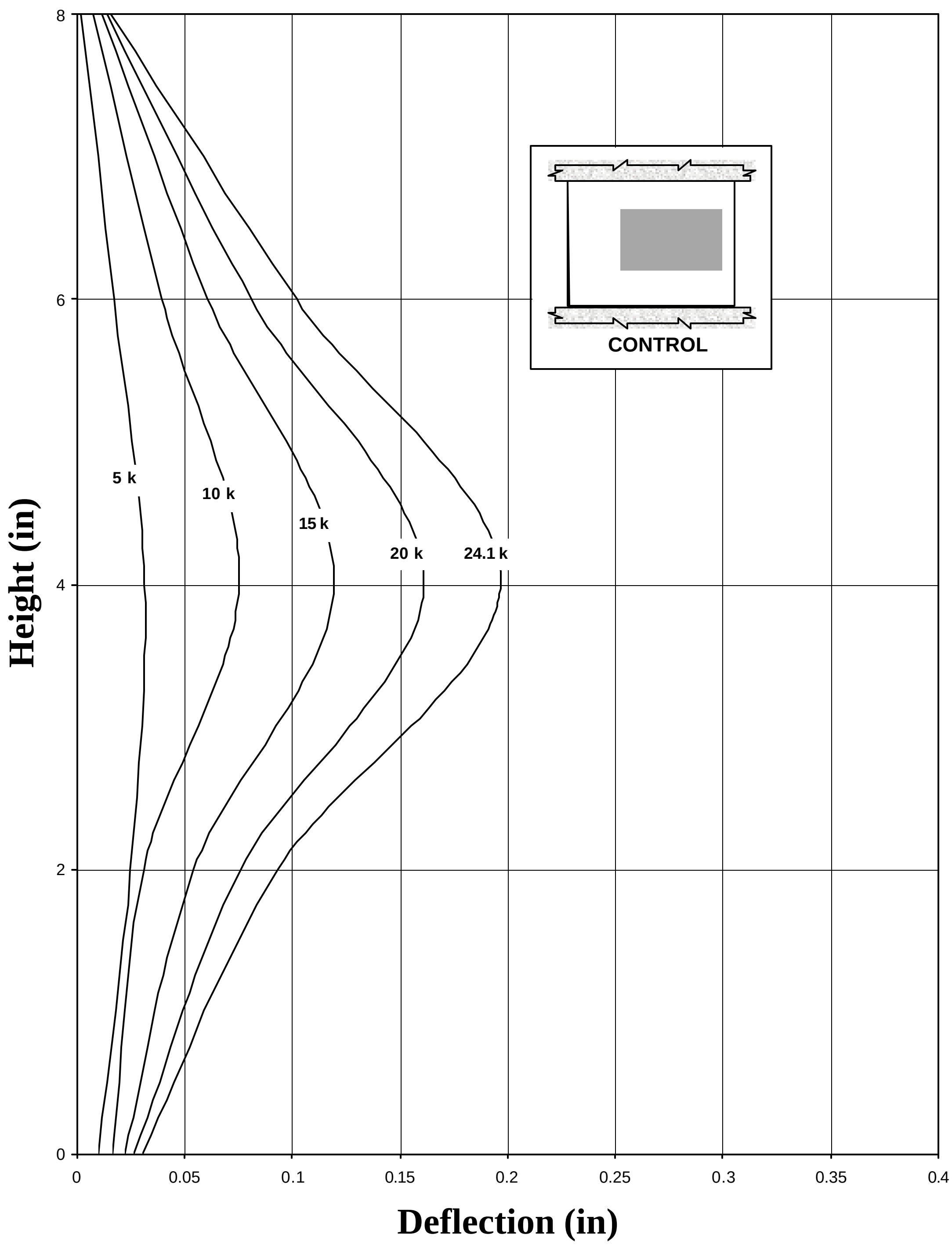

Figure C.6. Height vs. Deflection – Wall 2

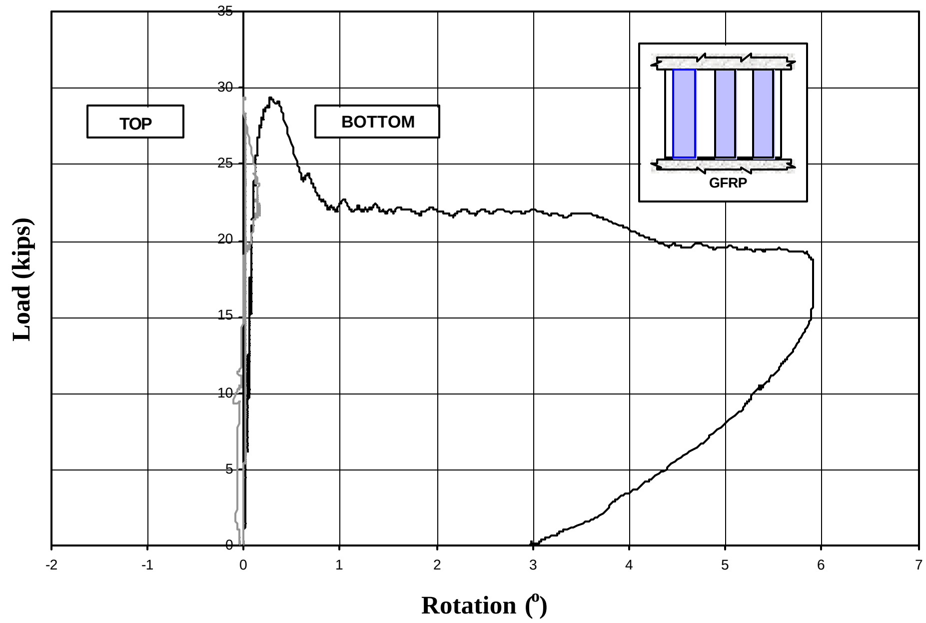

Figure C.7. Load vs. Rotation – Wall 3

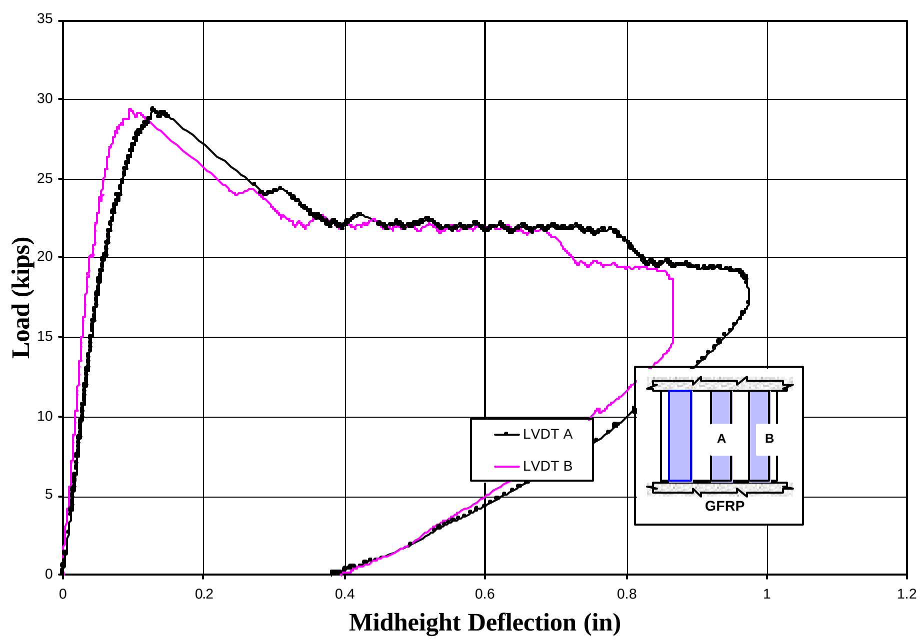

Figure C.8. Two- way action –Wall 3

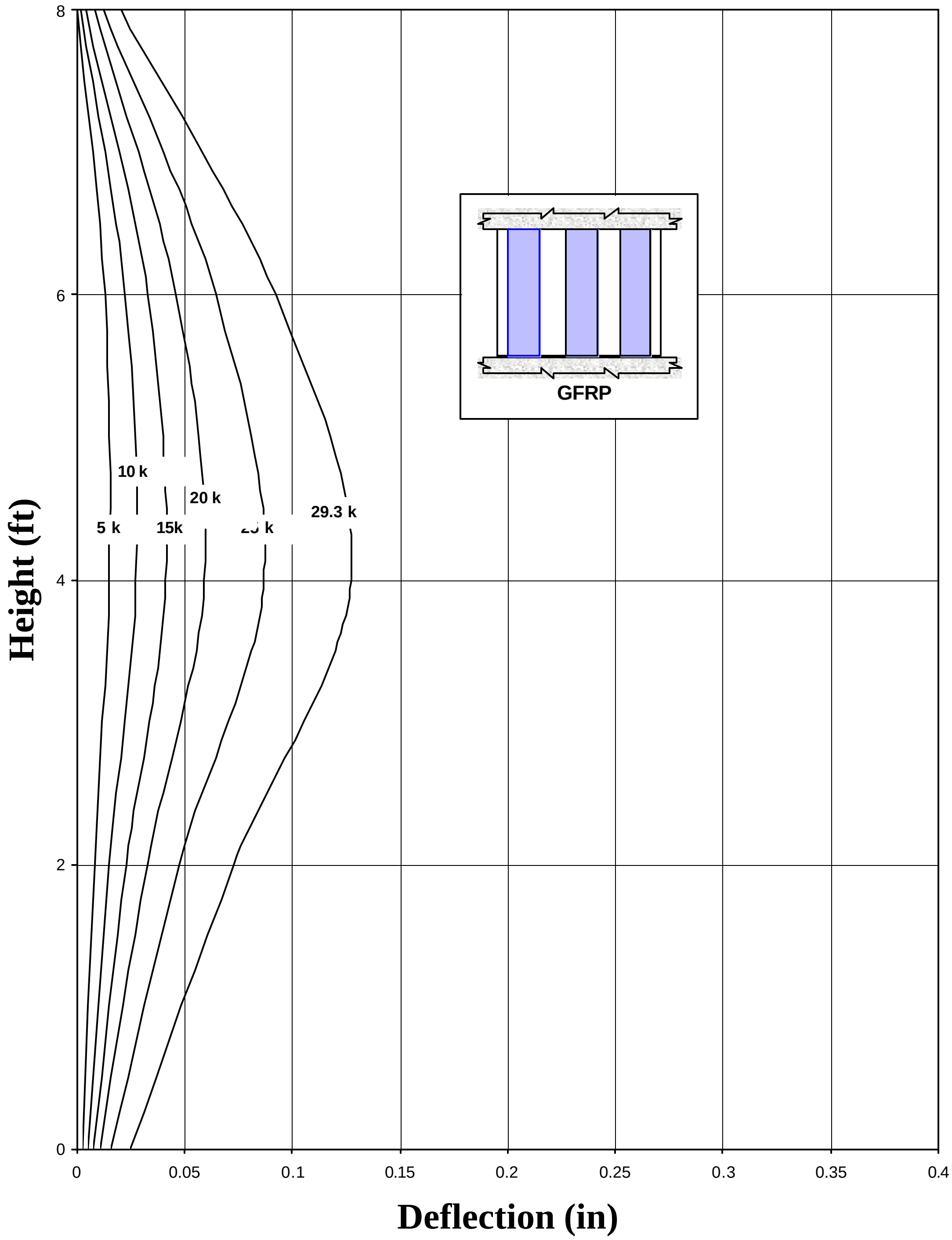

Figure C.9. Height vs. Deflection – Wall 3

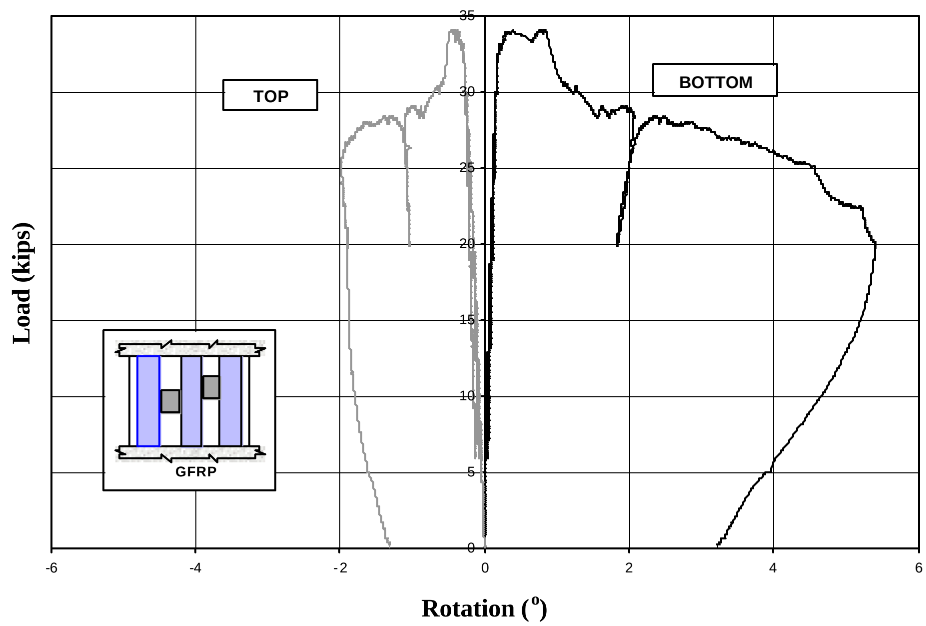

Figure C.10. Load vs. Rotation – Wall 4

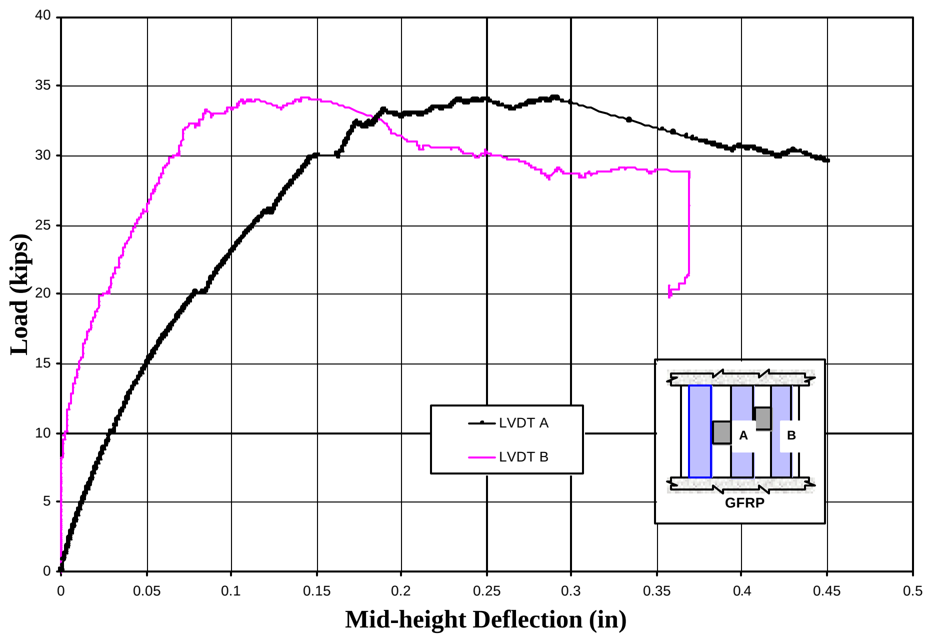

Figure C.11. Two- way action–Wall 4

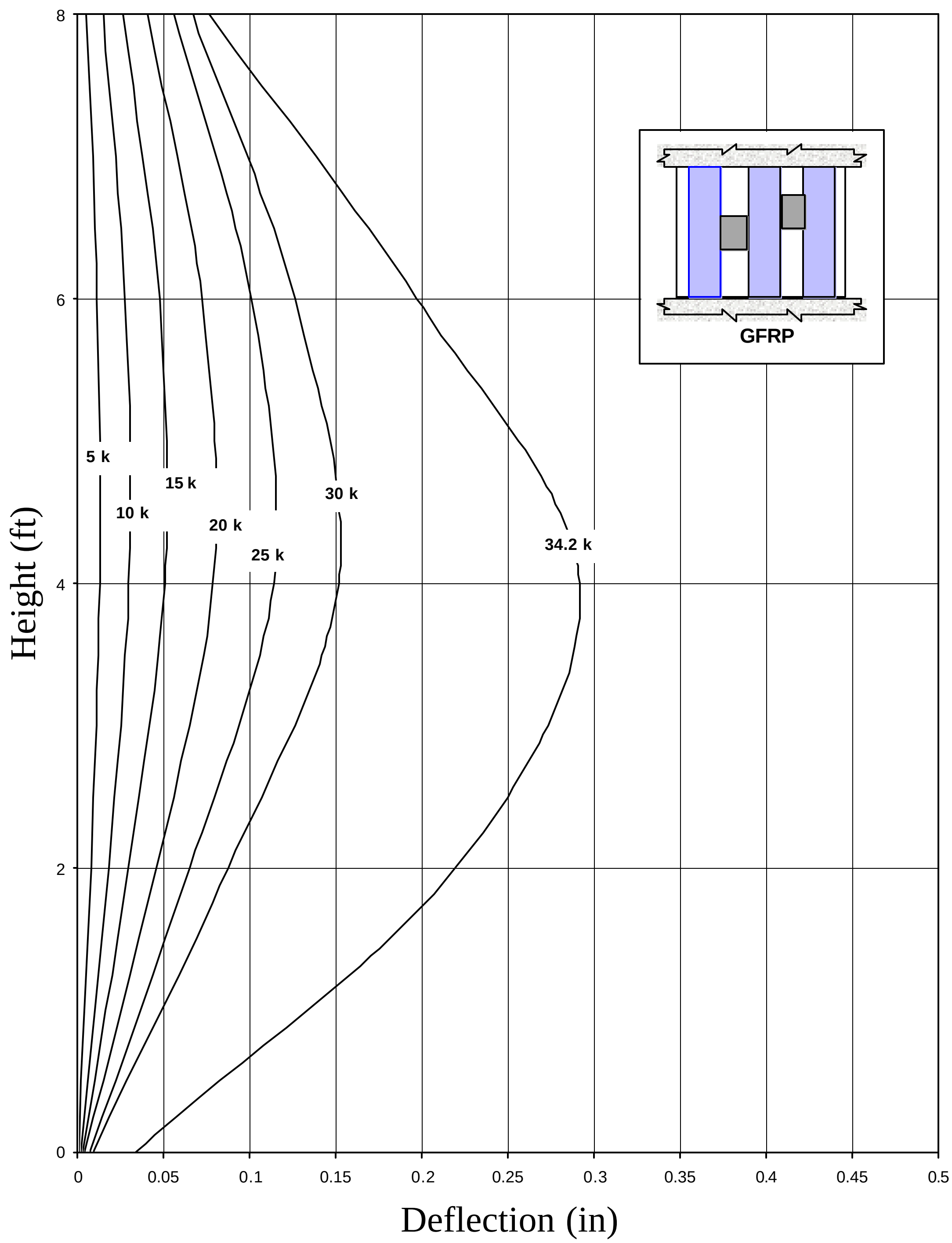

Figure C.12. Height vs. Deflection – Wall 4

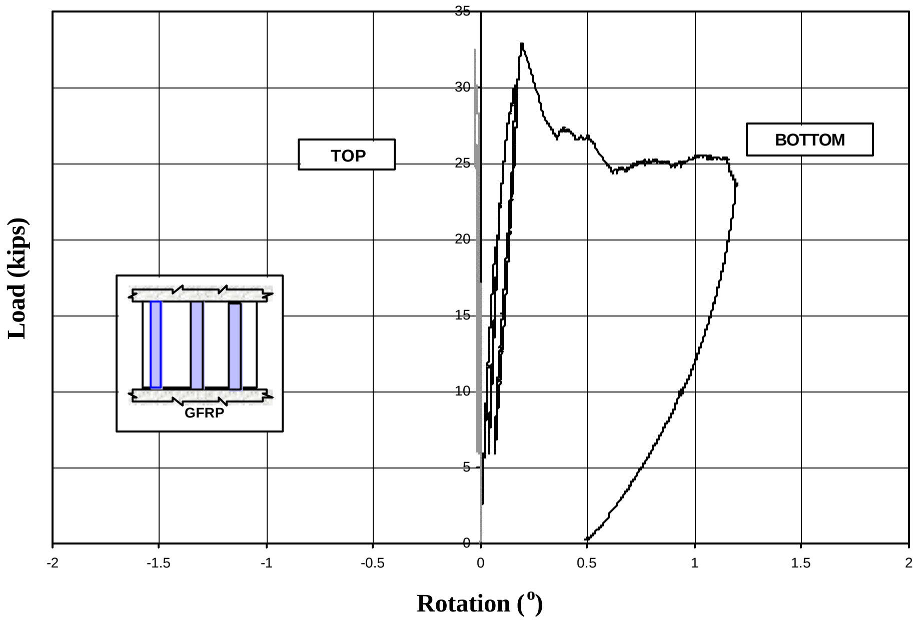

Figure C.13. Load vs. Rotation – Wall 5

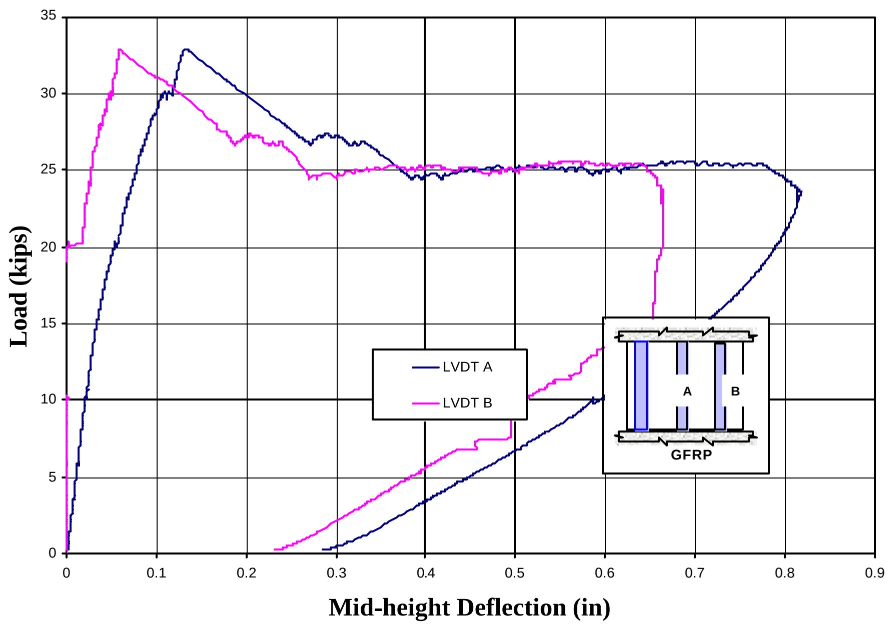

Figure C.14. Two- way action –Wall 5

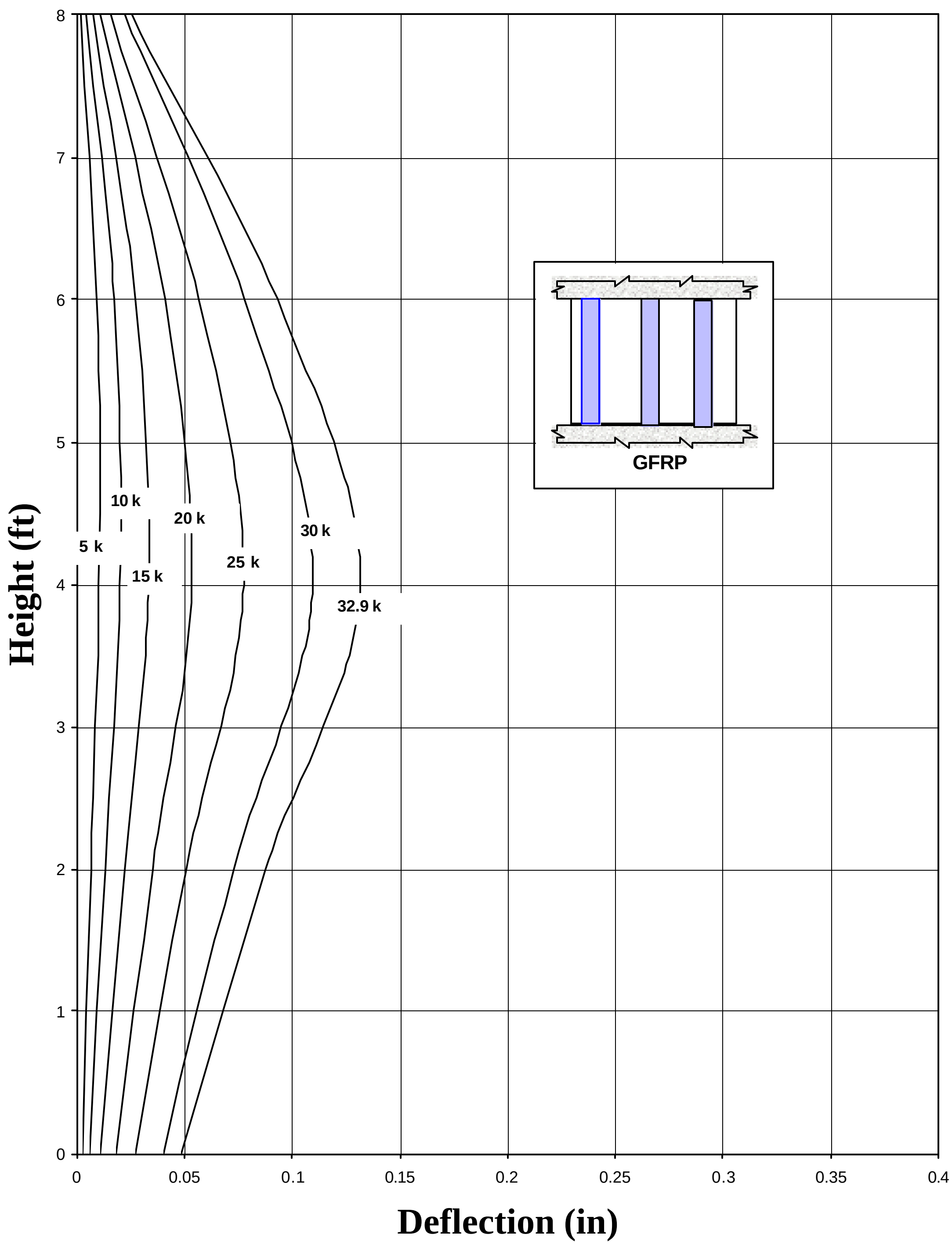

Figure C.15. Height vs. Deflection – Wall 5

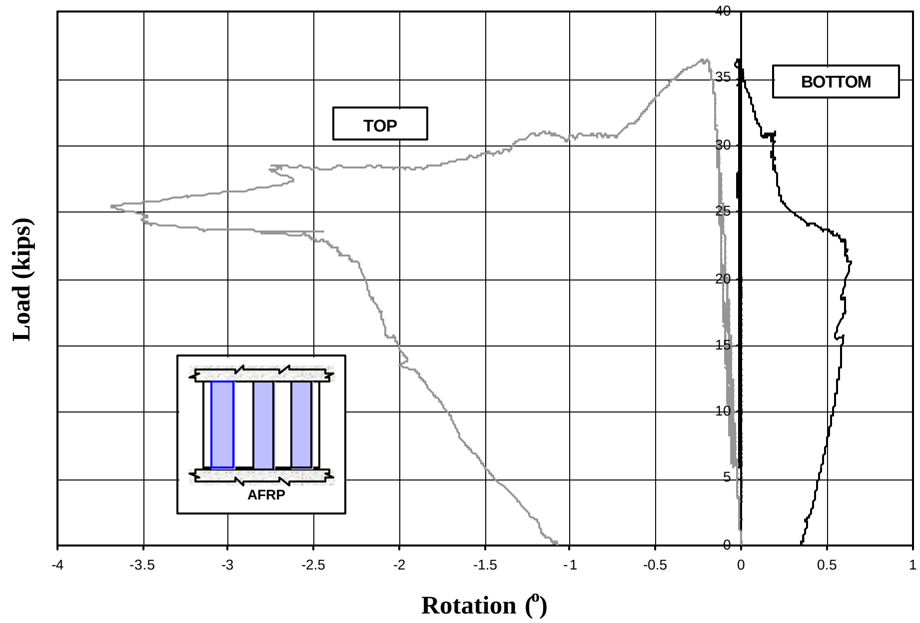

Figure C.16. Load vs. Rotation – Wall 6

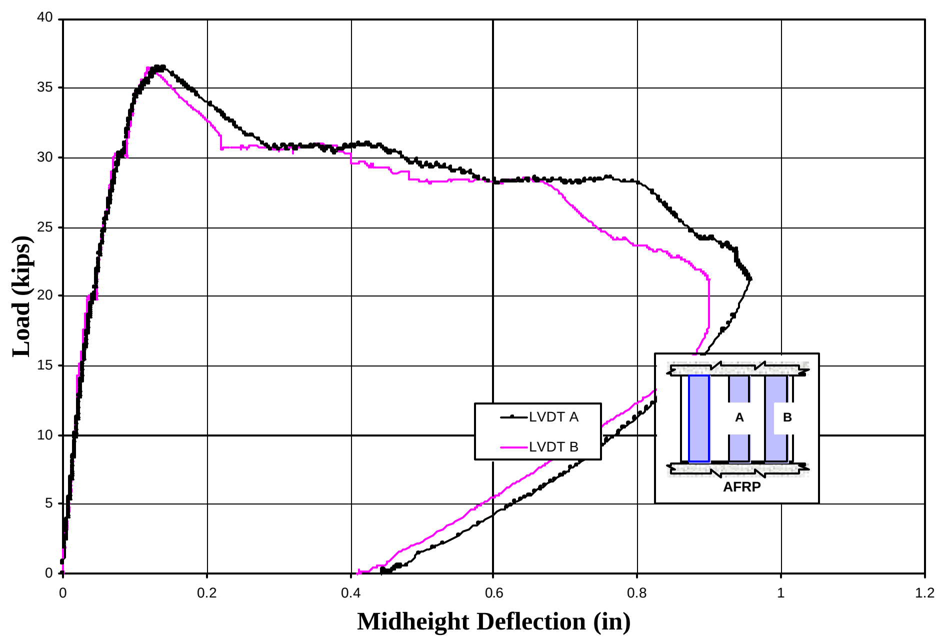

Figure C.17. Two- way action –Wall 6

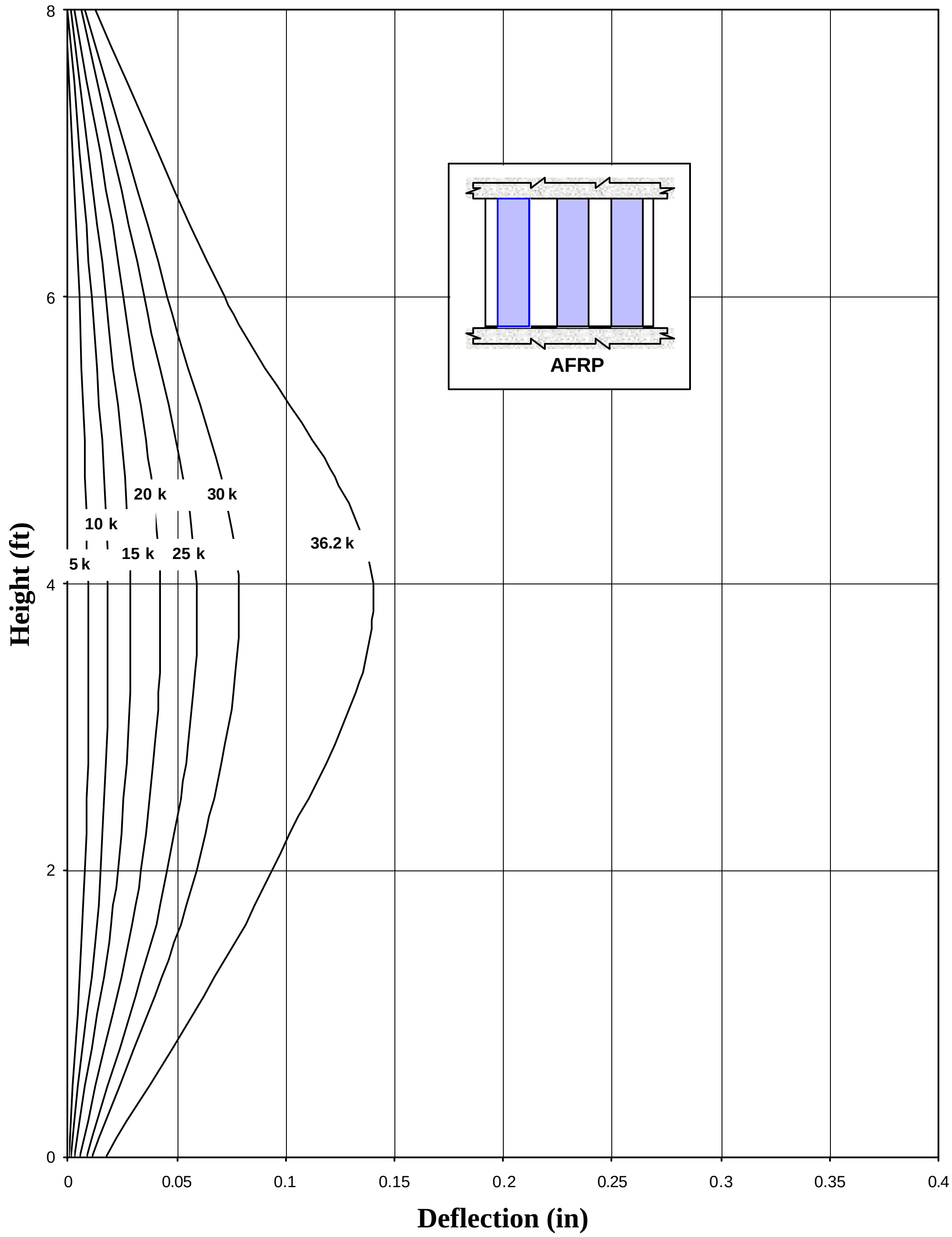

Figure C.18. Height vs. Deflection – Wall 6

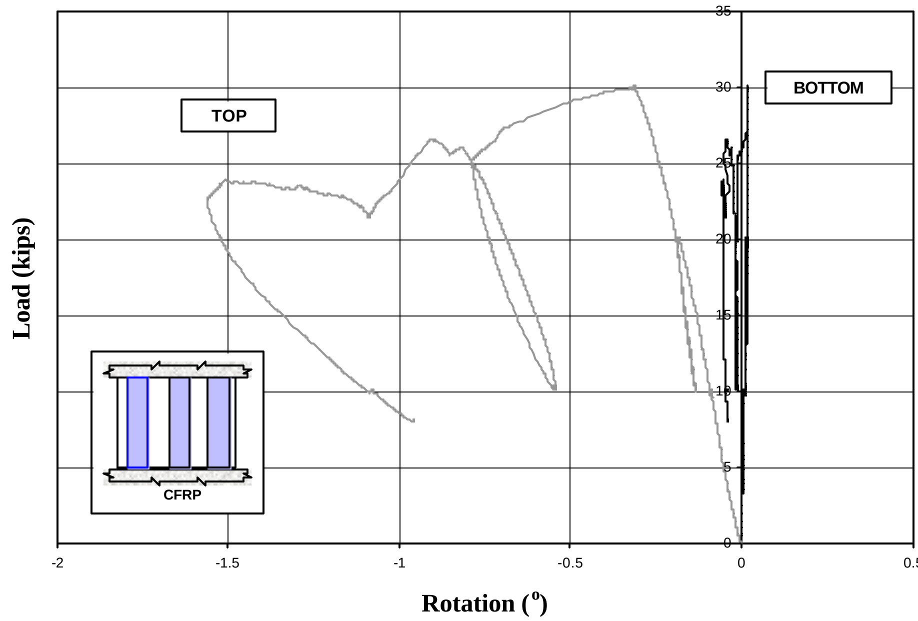

Figure C.19. Load vs. Rotation – Wall 7

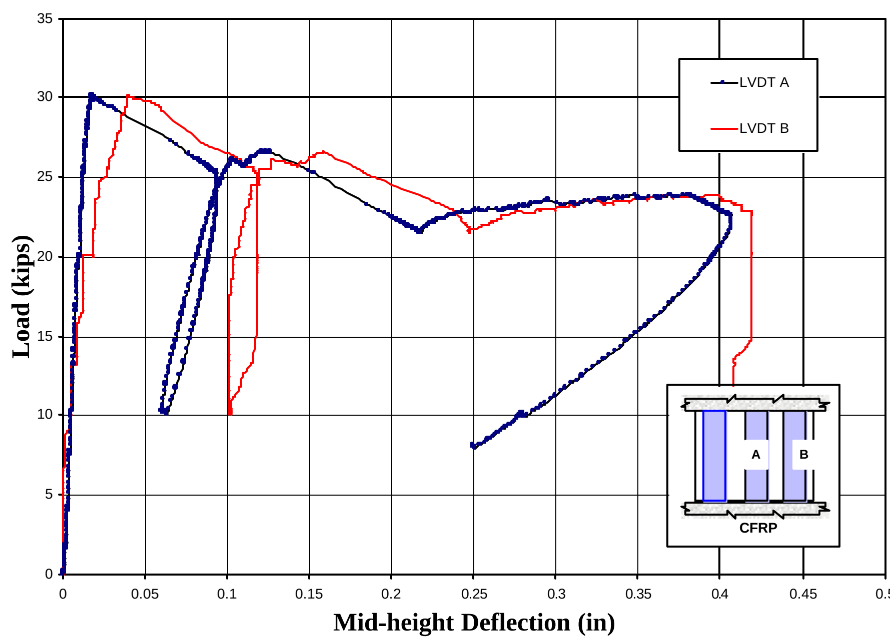

Figure C.20. Two- way action –Wall 7

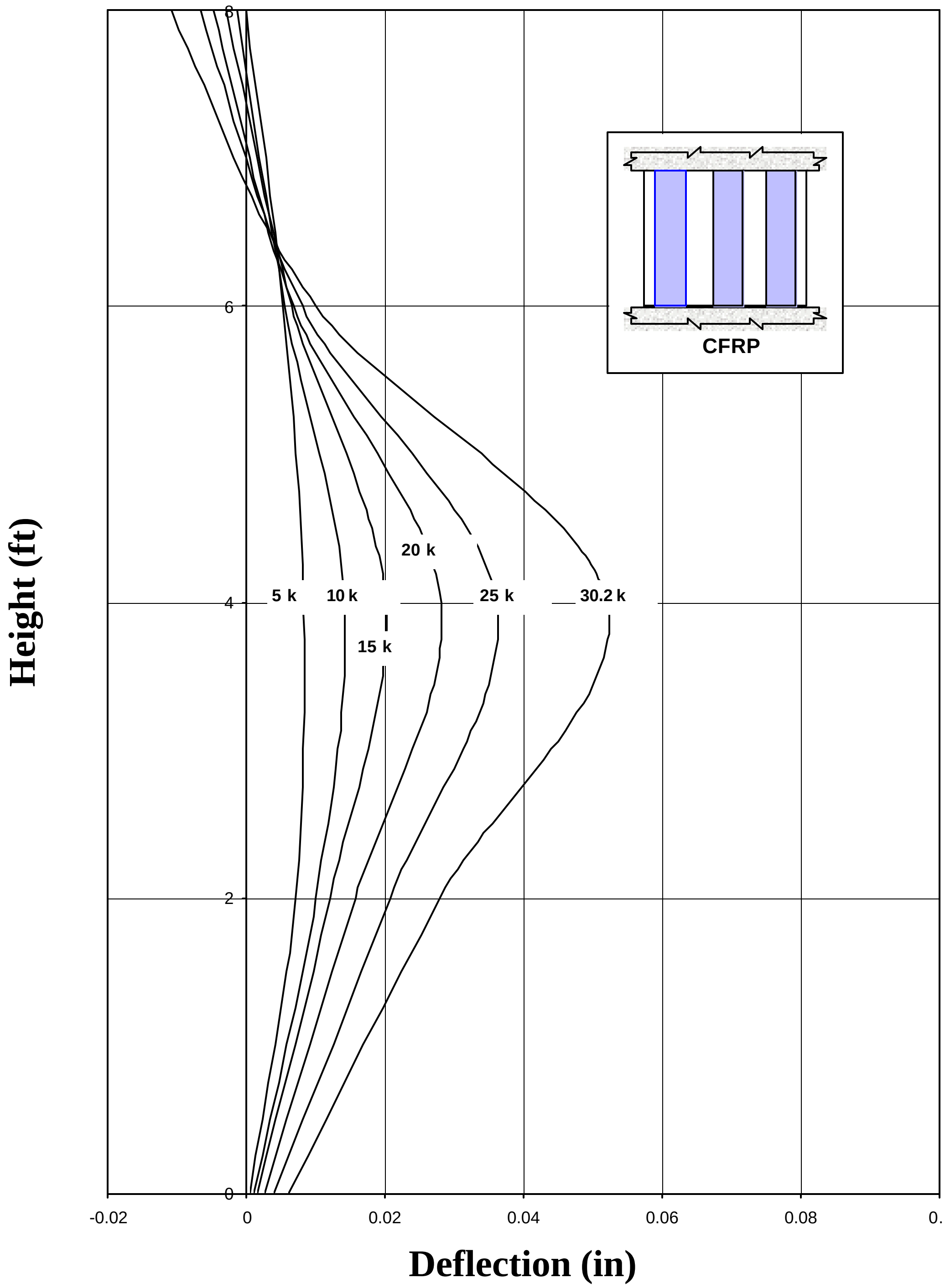

Figure C.21. Height vs. Deflection – Wall 7

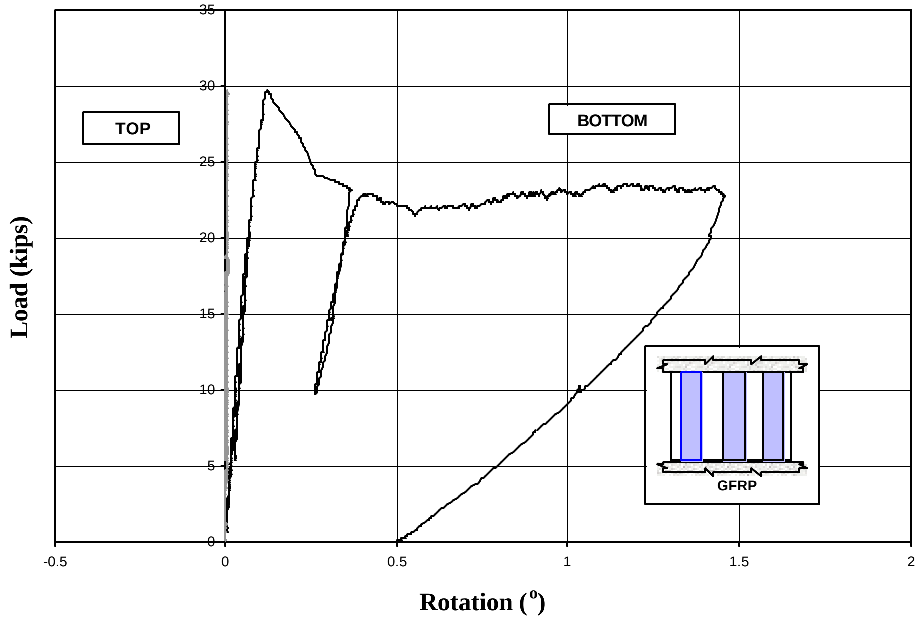

Figure C.22. Load vs. Rotation – Wall 8

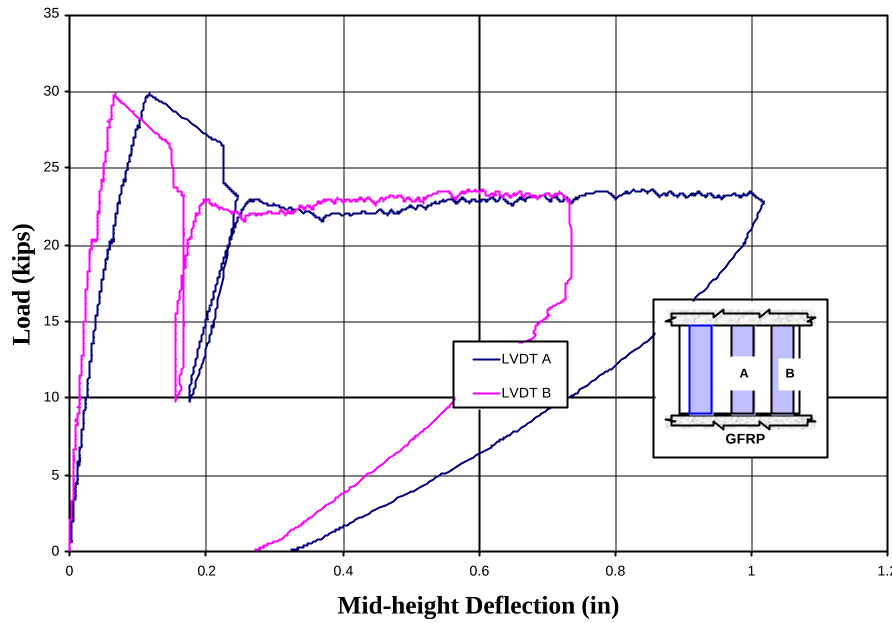

Figure C.23. Two- way action –Wall 8

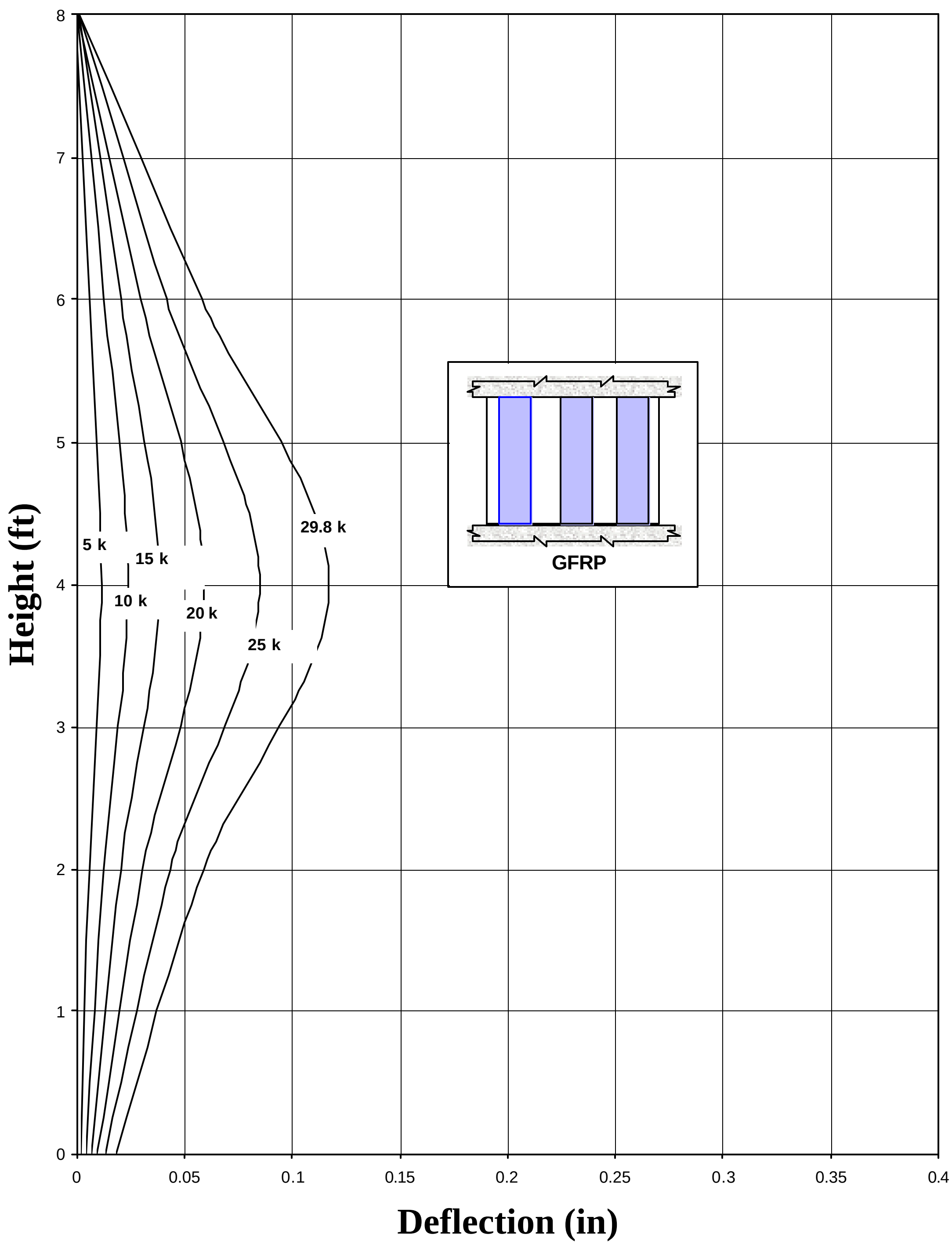

Figure C.24. Height vs. Deflection – Wall 8

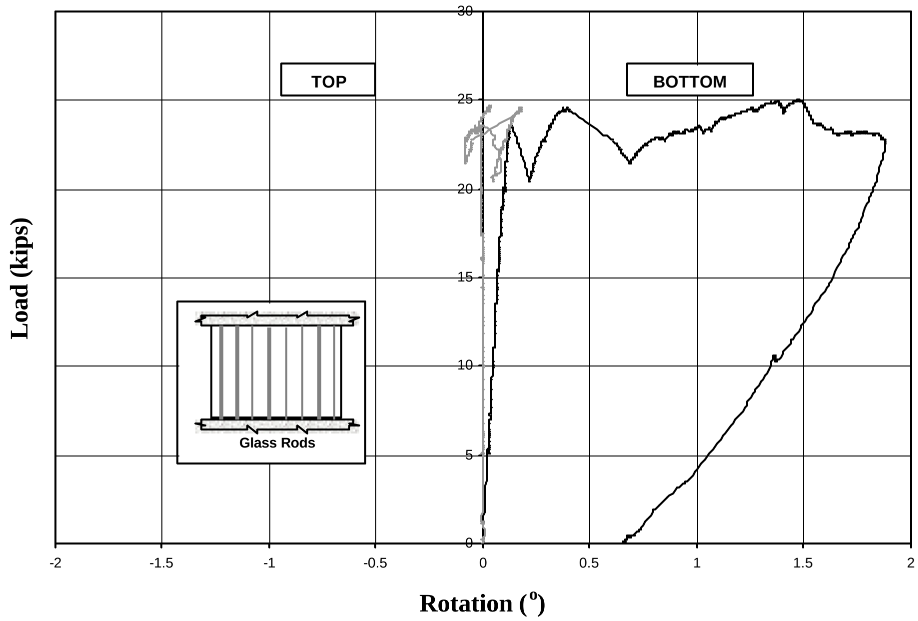

Figure C.25. Load vs. Rotation – Wall 9

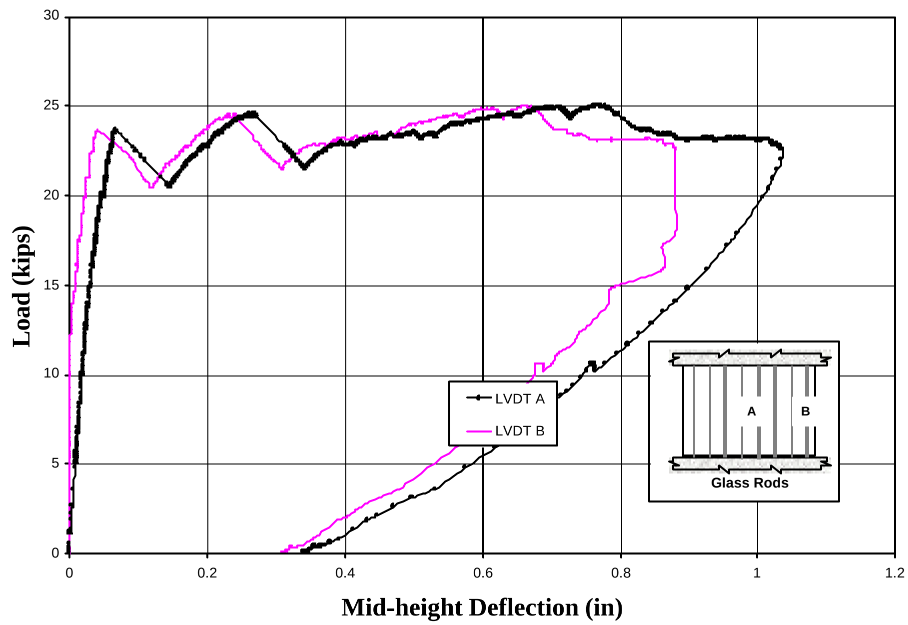

Figure C.26. Two- way action –Wall 9

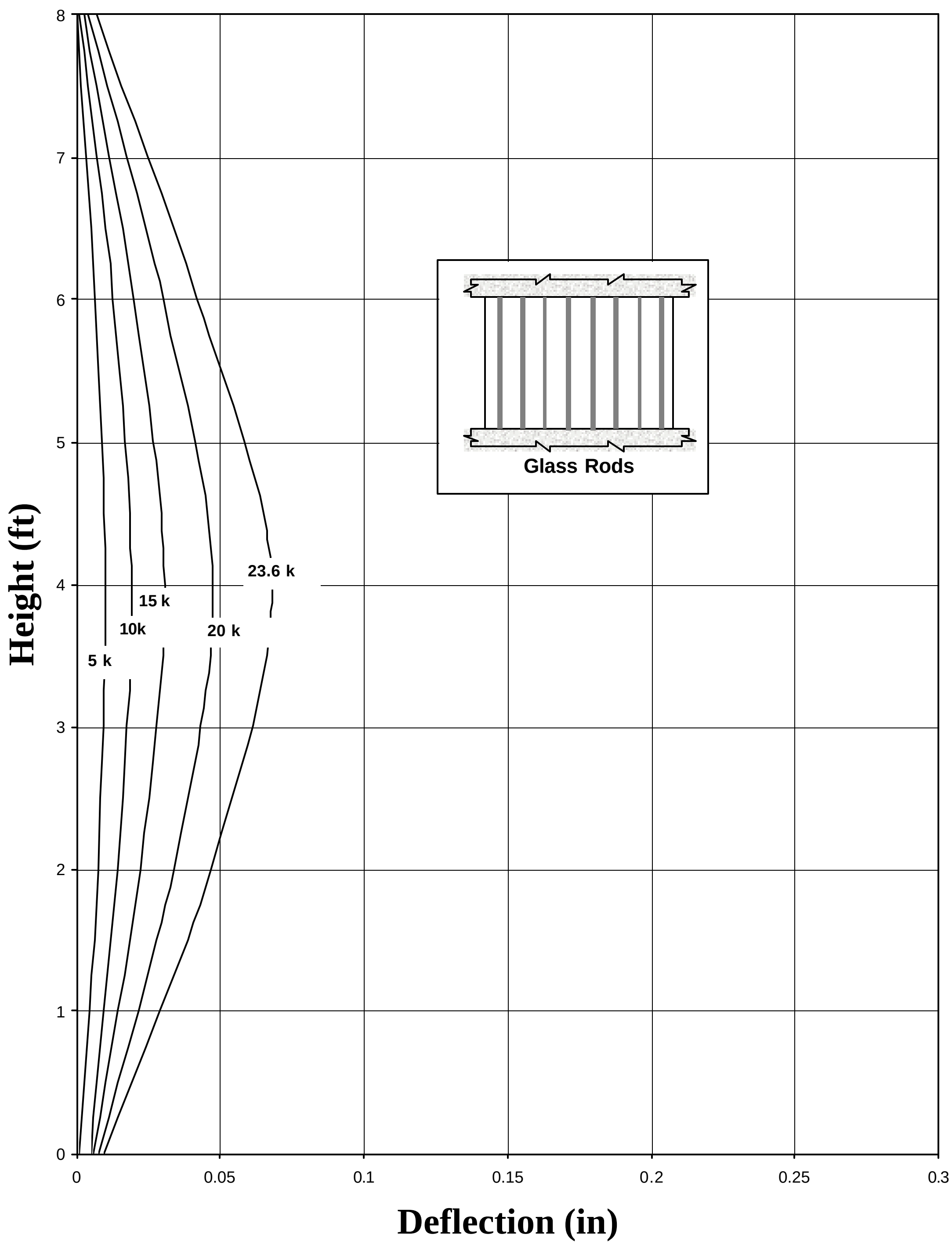

Figure C.27. Height vs. Deflection – Wall 9

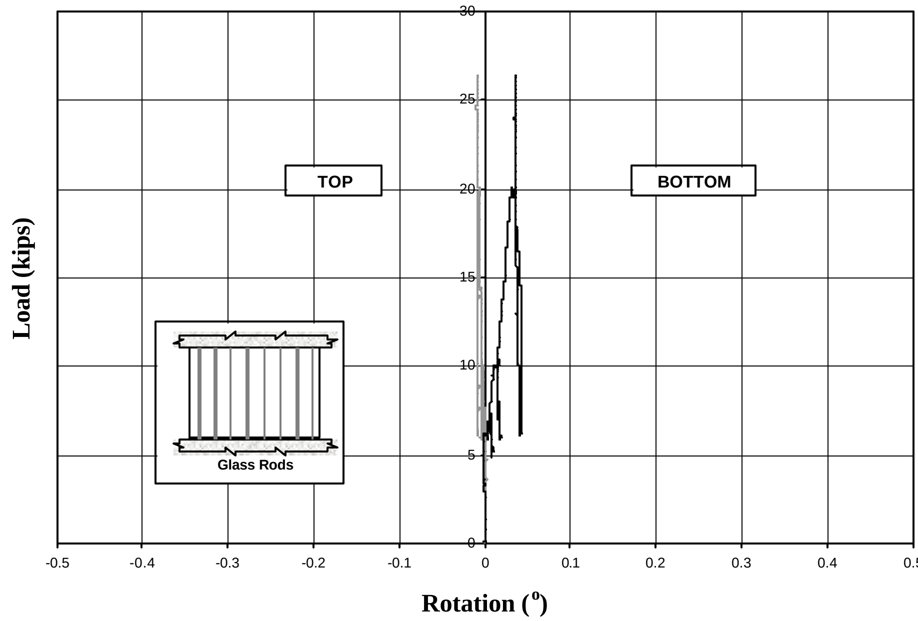

Figure C.28. Load vs. Rotation – Wall 10

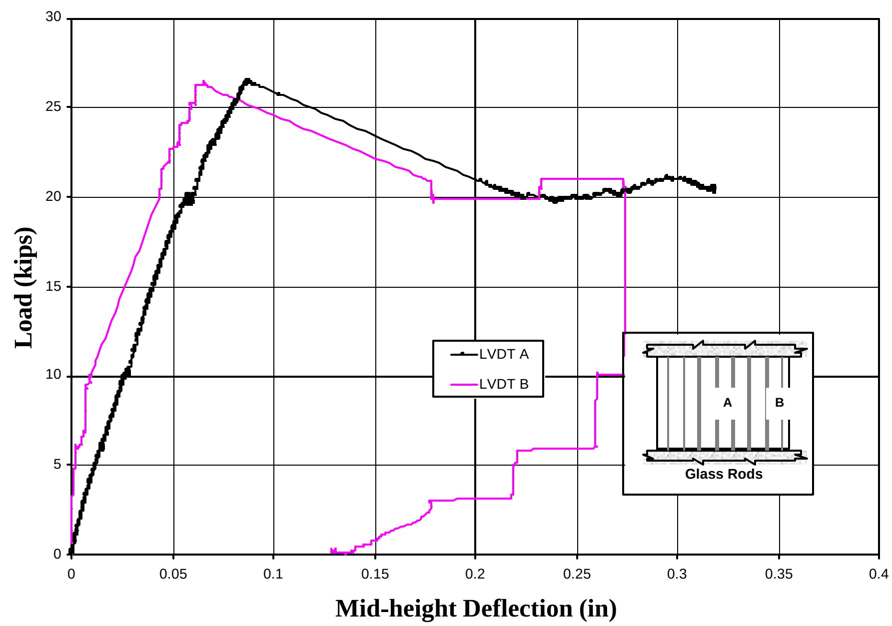

Figure C.29. Two- way action –Wall 10

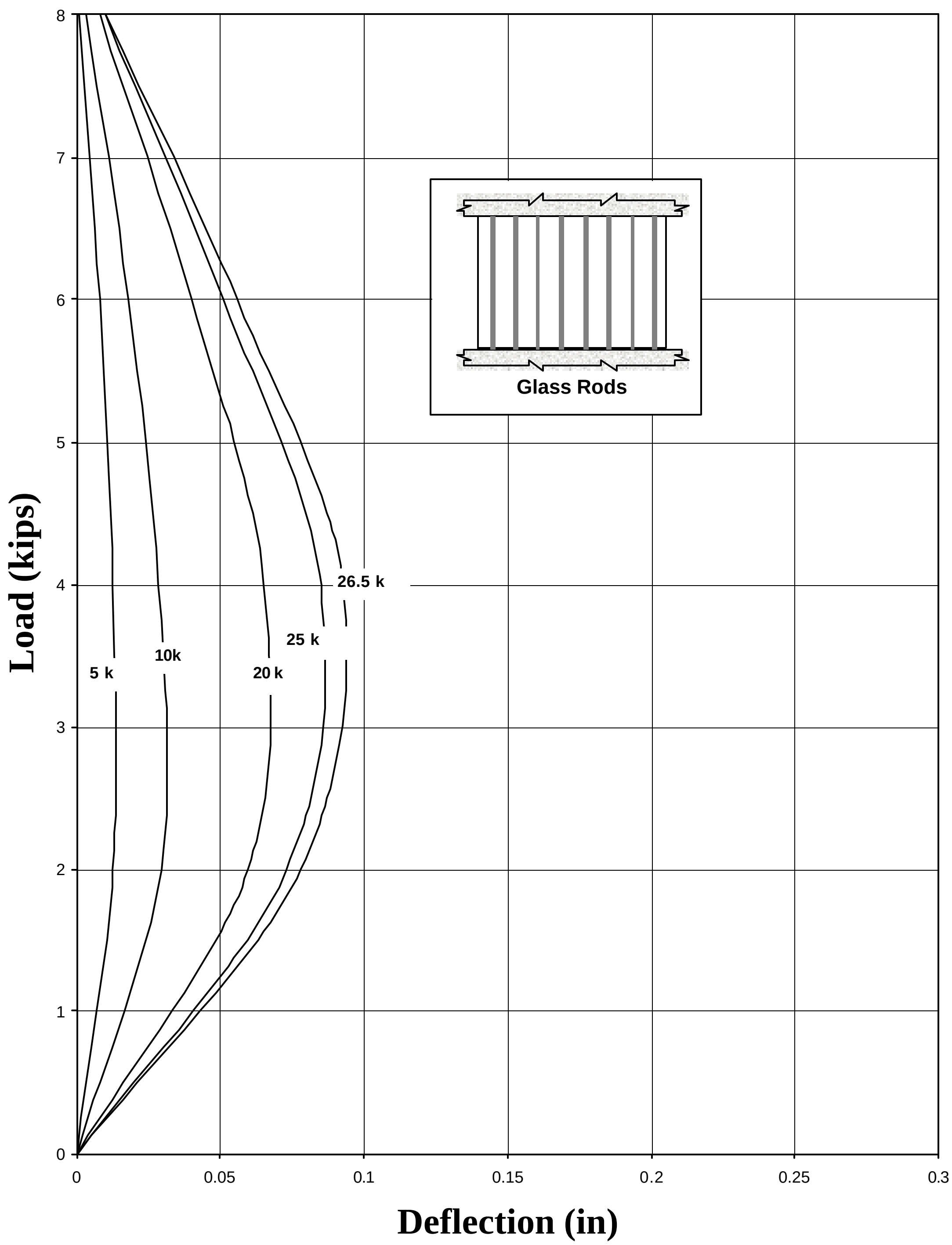

Figure C.30. Height vs. Deflection – Wall 10

APPENDIX D

IN-PLANE TEST RESULTS

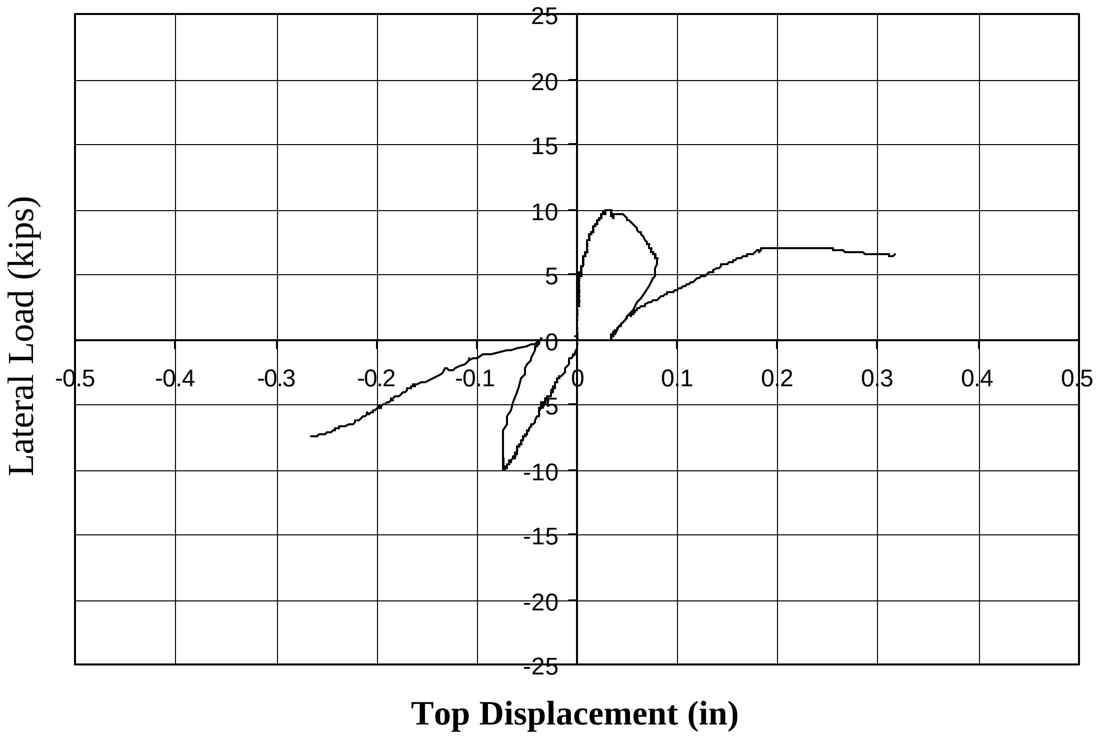

Figure D.1. Lateral Load vs. Top Displacement – Wall 1

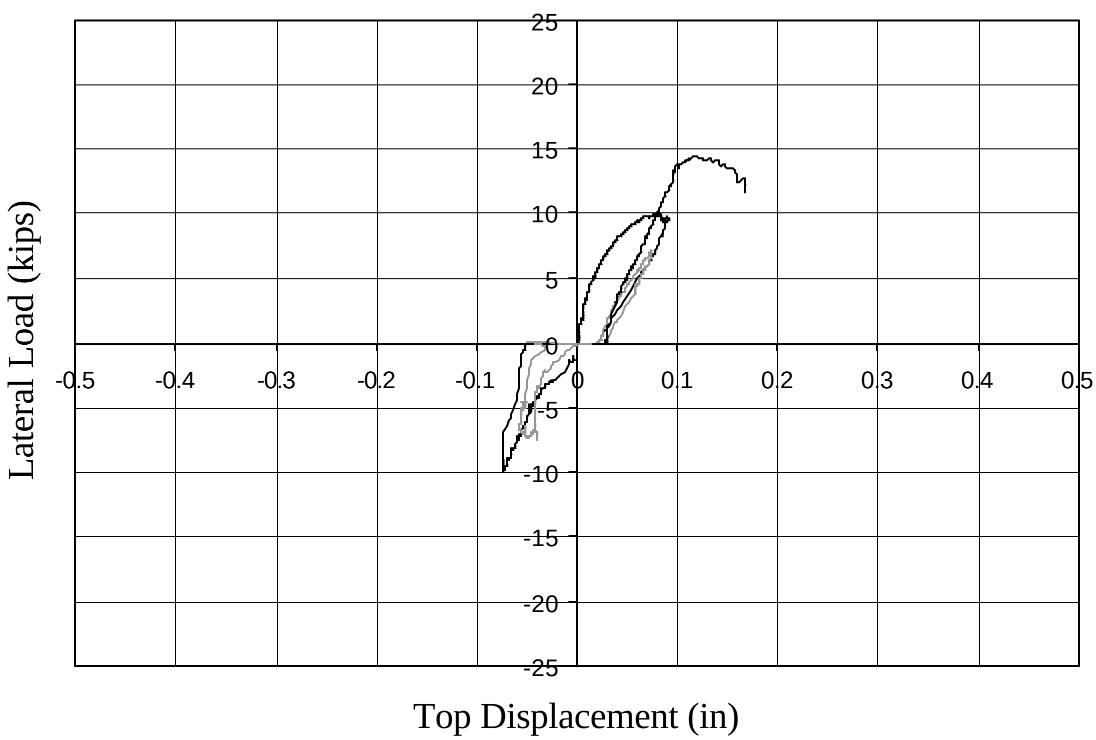

Figure D.2. Lateral Load vs. Top Displacement – Wall 2

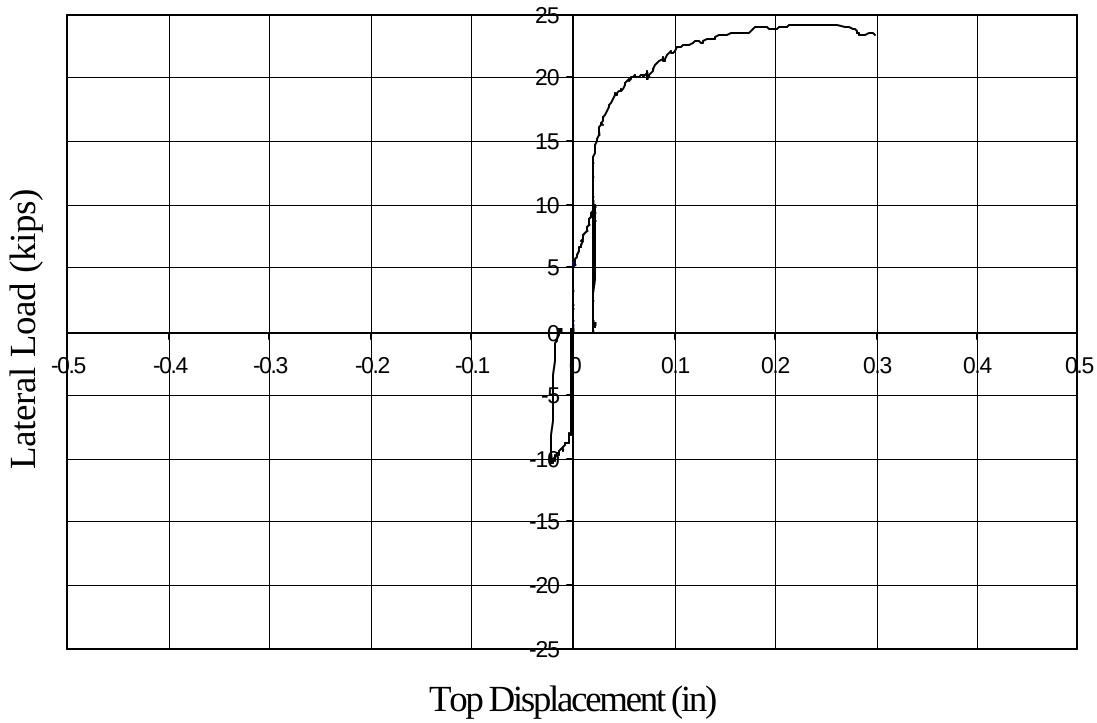

Figure D.3. Lateral Load vs. Top Displacement – Wall 3

REFERENCES

Johnson F.B., and Matthys J. H. (1973), “ Structural Strength of Hollow Clay Tile Assemblages,” Proceedings of the American Society of Civil Engineers – Journal of the Structural Division, February 1973, pp. 259-275.

Prawel S.P., and Reinhorn A.M. (1985), “Seismic Retrofit of Structural Masonry Using a Ferrocement Overlay,” Proceedings of the Third North American Masonry Conference, Arlington, Texas, June 1985, pp. 50-1 to 50-19.

Fricke K.E., Jones W.D., and Huff T.E. (1992), “In situ lateral Load Testing of Unreinforced Masonry Hollow Clay Tile Wall,” Proceedings of the Sixth Canadian Masonry Symposium, Saskatchewan, Canada, June 1992, pp. 519-530.

TMS (1994), “Performance of Masonry Structures in the Northridge California earthquake of January 17, 1994,” The Masonry Society.

Angel R., Abrams D.P., Shapiro D., Uzarski J., and Webster M. (1994), “Behavior of Reinforced Concrete Frames with Masonry Infills,” Structural Research Series Report No. 589, Department of Civil Engineering, University of Illinois at Urbana-Champaign, March 1994, 183 pp.

Schwegler G. (1995), “Masonry Construction Strengthened with Fiber Composites in Seismically Endangered Zones,” Proceedings of the Tenth European Conference on Earthquake Engineering, Rotterdam, 1995, pp.2299-2303.

Laursen P.T., Seible F., Hegemier G.A., and Innamorato D. (1995), “Seismic Retrofit and Repair of Masonry Walls with Carbon Overlays,” Non-Metallic (FRP) Reinforcement for Concrete Structures. Edited by L. Taerwe, RILEM, pp. 616-627.

Manzouri T., Shing P.B., Schuller M.P, and Atkinson R.H. (1996) “Strengthening of Unreinforced Masonry Buildings,” Proceedings of the Seventh North American Masonry Conference, Indiana, June 1996, pp. 839-852.

Hartley A., Mullins G., and Sen R. (1996), “Repair of Concrete Masonry Block Walls using Carbon Fiber,” Advanced Composite Materials in Bridges and Structures, Montreal, Quebec, 1996, pp. 795-802.

Schwegler G., and Kelterborn P. (1996), “Earthquake Resistance of Masonry Structures strengthened with Fiber Composites,” Eleventh World Conference on Earthquake Engineering, Acapulco, Mexico, 1996.

Benett R. M., Boyd K.A., and Flanagan R.D. (1997), “ Compressive Properties of Structural Clay Tile Prisms,” Proceedings of the American Society of Civil Engineers – Journal of Structural Engineering, July 1997, pp. 920-926.

Velazquez J.I., (1998), "Out-of-Plane Cyclic Behavior of URM Walls Retrofitted with Fiber Composites," Ph.D. Dissertation Department of Civil Engineering and Engineering Mechanics, The University of Arizona.

ACI-530-99/ASCE 5-99/TMS 402-99 (1999), "Masonry Standards Joint Committee – Code, Specification and Commentaries"

Drysdale R., Hamid A, and Baker L. (1999), Masonry Structures – Behavior and Design, The Masonry Society. Boulder, Colorado.

Roko K., Boothby T.E., and Bakis C.E., (1999), "Failure Modes of Sheet Bonded Fiber Reinforced Polymer Applied to Brick Masonry," Fourth International Symposium on Fiber Reinforced Polymer (FRP) for Reinforced Concrete Structures, Baltimore, Maryland, November 1999, pp. 305-311.

Hamilton H.R. III, Holberg A., Caspersen J., and Dolan C.W. (1999), "Strengthening Concrete Masonry with Fiber Reinforced Polymers," Fourth International Symposium on Fiber Reinforced Polymer (FRP) for Reinforced Concrete Structures, Baltimore, Maryland, November 1999, pp. 1103-1115.